ASTROBIOLOGY
Volume 17, Number 4, 2017

DOI: 10.1089/ast.2016.1539

Radiation-Driven Formation of Reactive Oxygen Species in Oxychlorine-Containing Mars Surface Analogues

Christos D. Georgiou,[1] Dimitrios Zisimopoulos,[1] Electra Kalaitzopoulou,[1] and Richard C. Quinn[2]

Abstract

The present study demonstrates that γ-radiolyzed perchlorate-containing Mars soil salt analogues (in a CO_2 atmosphere) generate upon H_2O wetting the reactive oxygen species (ROS) superoxide radical ($O_2^{\bullet-}$), hydrogen peroxide (H_2O_2), and hydroxyl radicals ($^{\bullet}OH$). This study also validates that analogue radiolysis forms oxychlorine species that, in turn, can UV-photolyze to $^{\bullet}OH$ upon UV photolysis. This investigation was made possible by the development of a new assay for inorganic-origin $O_2^{\bullet-}$ and H_2O_2 determination and by the modification of a previous assay for soil $^{\bullet}OH$. Results show that radiolyzed $Mg(ClO_4)_2$ generates H_2O_2 and $^{\bullet}OH$; and when included as part of a mixture analogous to the salt composition of samples analyzed at the Mars Phoenix site, the analogue generated $O_2^{\bullet-}$, H_2O_2, and $^{\bullet}OH$, with $^{\bullet}OH$ levels 150-fold higher than in the radiolyzed $Mg(ClO_4)_2$ samples. Radiolyzed Mars Phoenix site salt analogue that did not contain $Mg(ClO_4)_2$ generated only $^{\bullet}OH$ also at 150-fold higher concentration than $Mg(ClO_4)_2$ alone. Additionally, UV photolysis of the perchlorate γ radiolysis product chlorite (ClO_2^-) generated the oxychlorine products trihalide (Cl_3^-), chlorine dioxide ($ClO_2^{\bullet}$), and hypochlorite (ClO^-), with the formation of $^{\bullet}OH$ by UV photolysis of ClO^-. While the generation of ROS may have contributed in part to $^{14}CO_2$ production in the Viking Labeled Release (LR) experiment and O_2 (g) release in the Viking Gas Exchange (GEx) experiment, our results indicate that they are not likely to be the major contributor to the LR and GEx results. However, due to their highly reactive nature, they are expected to play a significant role in the alteration of organics on Mars. Additionally, experiments with hypochlorite show that the thermal stability of NaClO is in the range of the thermal stability observed for thermally liable oxidant responsible for the Viking LR results. Key Words: Mars—Oxygen—Salts—Radiation—Habitability. Astrobiology 17, 319–336.

1. Introduction

Currently, 40 years after the launch of the Viking Mission and the first search for extant life on Mars, the parent species in the planet's surface material that were responsible for the results of the Viking Gas Exchange (GEx) and Labeled Release (LR) experiments have not been definitely identified. In the GEx experiment, oxygen measured as O_2 (g) was released into the sample cell headspace when martian surface material was either humidified or wetted with an aqueous nutrient medium. The amount of O_2 (g) measured ranged from 70 to 700 nmol from the 1 cc samples that were tested, and this response persisted, at apparently reduced levels, in samples that were heat-treated to 145°C or stored at ~10°C for 160 sols (Oyama and Berdahl, 1977). In the LR experiment, when 0.5 cm^3 of surface soil material was wetted with an aqueous nutrient medium that contained ^{14}C-labeled organics, ~30 nmol of ^{14}C-labeled gas (presumably $^{14}CO_2$) was released into the LR test cell headspace (Levin and Straat, 1977). The LR response appeared to be more labile than the GEx response, did not survive heat treatment to 160°C, was significantly reduced by heat treatment for 3 h at 47°C and 51°C, and was eliminated by storage at 10–26°C for 141 sols. The results of the GEx and LR experiments, combined with the results of the Viking Gas Chromatograph Mass Spectrometer (GCMS) analyses, which appeared to show severely depleted levels of organics in the surface materials (Biemann *et al.,* 1977), led to the conclusion that the martian surface material contained at least three different oxidants (Klein *et al.,* 1976).

Initial interpretations of the Viking results focused on possible UV-induced formation of H_2O_2 and metal superoxides as the thermally unstable LR and the thermally stable GEx oxidant, respectively (Oyama *et al.,* 1977). The

[1]Department of Biology, University of Patras, Patras, Greece.
[2]Exobiology Branch, NASA Ames Research Center, Moffett Field, California, USA.

UV-induced formation of superoxide radicals ($O_2^{\bullet-}$) on anatase has been suggested as a source of the GEx oxidant (Chun *et al.,* 1978), as has UV-induced formation of $O_2^{\bullet-}$ on labradorite (Yen *et al.,* 2000). Complexation of H_2O_2 with anatase has also been suggested as another potential mechanism for the formation of the GEx oxidant (Quinn and Zent, 1999). More recent experiments, while not demonstrating capability with the LR and GEx results, have shown the formation of peroxide, superoxide, and other forms of reactive oxygen species (ROS), when Atacama Desert and Mojave Desert soils were exposed to UV radiation (Georgiou *et al.,* 2015). In these experiments, it was shown that these desert soils generate and can accumulate metal superoxides and peroxides by a UV-induced electron transfer mechanism, which involves electron ejection from metal oxides to O_2. Additionally, it was demonstrated in the dark that transformation of the UV-generated peroxide and superoxides can result in the generation of hydroxyl radicals ($^{\bullet}OH$).

New insight into the oxidative nature of the martian surface material was obtained with the discovery of perchlorate anions (ClO_4^-; likely as salts of Ca^{2+} and/or Mg^{2+}) by way of the Wet Chemistry Laboratory on the Phoenix Mars lander (Hecht *et al.,* 2009). Following the Phoenix mission, reinterpretation of the Viking GCMS results indicates the presence of perchlorate at both Viking landing sites (Navarro-González *et al.,* 2010); and analyses of surface materials, including ancient sedimentary deposits, with the Sample Analysis at Mars (SAM) instrument suite have shown that the perchlorate is widely distributed at the Mars Science Laboratory landing site (Glavin *et al.,* 2013; Ming *et al.,* 2014). Analyses of spectral data from the Compact Reconnaissance Imaging Spectrometer for Mars (CRISM) instrument show evidence for the seasonal presence of hydrated perchlorate at recurring slope lineae locations (Ojha *et al.,* 2015). Combined, these results are indicative of global perchlorate distributions on Mars and suggest that the martian surface contains a significantly higher level and more diverse range of oxidants than what was suggested by the Viking biology experiments of 40 years ago.

Given the high levels of UV radiation, galactic cosmic rays, and solar energetic particles that reach the martian surface (Catling *et al.,* 1999; Cockell *et al.,* 2000; Pavlov *et al.,* 2002; Hassler *et al.,* 2014), attention has turned to the potential role of radiation in the formation and alteration of oxychlorine species, including perchlorate, on Mars (Catling *et al.,* 2010; Quinn *et al.,* 2013; Carrier and Kounaves, 2015). In the context of the Viking biology experiments, it was shown in a study using calcium perchlorate exposed to γ rays in a CO_2 atmosphere that the LR results could be explained by the spontaneous decomposition of chloroaniline formed by the reaction of hypochlorite (formed through perchlorate radiolysis) with alanine in the LR nutrient media (Quinn *et al.,* 2013). This study also showed that, upon humidification or wetting, O_2 (g) is measured upon dissolution of perchlorate salts, presumably from trapped oxygen within the radiation-damaged perchlorate (Quinn *et al.,* 2013).

In the present study, we quantified the distributions of ROS produced in magnesium perchlorate and a Mars analog salt mixture by exposure to γ radiation using a new method for measurement of $O_2^{\bullet-}$ and H_2O_2 and a previously developed assay for soil $^{\bullet}OH$. Photochemical processing of the analogues was also examined to evaluate other potential mechanisms of ROS production in the martian surface environment. Quinn *et al.* (2013) quantified distributions of oxychlorine species produced in γ-irradiated perchlorate samples and demonstrated that these samples release O_2 (g) in a manner similar to what was observed in the Viking GEx experiment. However, in contrast to the oxychlorine content, Quinn *et al.* (2013) did not identify the chemical state and reactivity of the oxygen in these types of samples. In the present study, we examined the production of ROS in perchlorate-containing Mars surface analogues to provide another dimension to the current understanding of the reactive nature of the Viking samples. While Quinn *et al.* (2013) showed that the results of the primary release of CO_2 in the LR experiment could be explained by the presence of hypochlorite, the nature of the oxygen produced and its relationship to the GEx experiment were not fully explored. In addition to offering insight into the results of the GEx experiment, the production of ROS in martian surface material and its high oxidative reactivity potentially have important implications for our understanding of the preservation and detection of biomarkers on Mars.

2. Materials and Methods

2.1. Reagents

Acetonitrile (ACN, HPLC grade cat. # 34998), hydrogen peroxide solution (H_2O_2 30%, cat. # H1009), xylenol orange (XO, Na_4-salt, cat. # X3500), ferrous ammonium sulfate hexahydrate (FAS, cat. # 215406), catalase (CAT, cat. # C3155), dimethyl sulfoxide (DMSO, cat. # 472301), potassium superoxide (KO_2, cat. # P0647), sodium chlorite ($NaClO_2$, cat. # 244155), magnesium peroxide (MgO_2, cat. # 63130), sodium peroxide (Na_2O_2, cat. # 311456), and hydroethidine (HE, cat. # D7008) were obtained from Sigma-Aldrich (St. Louis, MO, USA). D-Sorbitol (anhydrous, cat. # 194742) was obtained from MPI Biochemicals (Santa Ana, CA, USA). Calcium peroxide (CaO_2, cat. # 21157), dicyclohexano-18-crown-6 ether (CE, cat. # A15344), ascorbic acid (cat. # 36237), and terephthalic acid (TPA, cat. # 43423) were obtained from Alfa Aesar (Karlsruhe, Germany). Sodium hypochlorite solution (NaClO, cat. # 105614) and $CuSO_4 \cdot 5H_2O$ (cat. # 102787) were obtained from Merk (Darmstadt, Germany). All other chemicals used in this study were reagent grade.

2.2. Preparation of perchlorate samples

The Mars Phoenix salt analogue is chemically analogous to the 80 mg water-soluble salts detected per 1 cc of martian soil and is described by Quinn *et al.* (2011). This analog mixture includes 58.3 μmol ClO_4^- and is referred to as the complete analogue. A second version of this analogue, which does not contain perchlorate, is referred to as the incomplete salt analogue (Quinn *et al.,* 2011). Gamma irradiation (500 kGy) was performed as described by Quinn *et al.* (2013), using samples sealed in glass ampules under 7.5 mbar CO_2 to simulate the martian atmosphere (Table 1).

2.3. Inorganic-origin superoxide ($O_2^{\bullet-}$) and peroxide (H_2O_2) assay

A new assay for the simultaneous determination of $O_2^{\bullet-}$ and H_2O_2 generated from the Mars Phoenix analogues was developed to study the possible γ-radiation production of

TABLE 1. H_2O_2, $O_2^{\bullet-}$ AND $^{\bullet}OH$ GENERATED BY RADIOLYZED $Mg(ClO_4)_2$ AND MARS PHOENIX SITE SALT ANALOGUE

ROS formed		*H_2O_2[a]; $O_2^{\bullet-}$[b]*			*$^{\bullet}OH$[c]*		
Samples	*Extraction treatment*	*Unheated*	*Heated*	*Fold*[a]	*Unheated*	*Heated*	*Fold*[a]
1. $Mg(ClO_4)_2$ (6.5 mg, or 58.3 μmol ClO_4^-)	ACN-solid solution[d]	6.27[a]; 0[b] (0.011[a]; 0[b])	0.1[a]; 0[b] (0.00017[a]; 0[b])	61↓	1.01 (0.0017)	6.93 (0.012)	6.9↑
2. Incomplete salt analogue (73.5 mg)	i. ACN-extract[e]	0[a]; 0[b]	0[a]; 0[b]	—	147	50	2.9↓
	ii. ACN/H_2O-solid extract[e]	0.57; n/a	0.18; n/a	3.2↓			
Sample 1 + 2 sum		6.84	0.28	**24**↓	148	56.9	**2.6**↓
3. Complete salt analogue: $Mg(ClO_4)_2$ (6.5 mg) + incomplete salt analogue (73.5 mg)[b]	i. ACN-extract[c]	1.95[a]; 1.0[b] (0.0033[a]; 0.002[b])	0.60[a]; 0[b] (0.001[a]; 0[b])	3.3↓			
	ii. ACN/H_2O-solid extract[e]	0.63; n/a (~0.001; n/a)	0.71; n/a (~0.001; n/a)	—	149	75	**2**↓
		..... sum[f] = **3.1**	..... sum[f] = **1.31**	..... **2.3**↓			

[a,b,c]Concentrations of H_2O_2, $O_2^{\bullet-}$, and $^{\bullet}OH$ are expressed in nmol per indicated mg of sample. The concentration values in parentheses are mol % expressed in, *e.g.,* nmol produced from 100 nmol of radiolyzed ClO_4^-, where 100% corresponds to the 58.3 µmol ClO_4^- contained in the 6.5 mg radiolyzed $Mg(ClO_4)_2$. Fold changes of heated over unheated are shown with upward (fold increase) and downward (fold decrease) arrows.

[b]$O_2^{\bullet-}$ is determined only in the ACN_{alk}-CE extract of the samples as dictated by the employed $O_2^{\bullet-}$ assay. $O_2^{\bullet-}$ nmol are derived from the quantified nmol of H_2O_2 that are released from $O_2^{\bullet-}$ dismutation, which are multiplied by a factor of 2 [according to the stoichiometry of the dismutation reaction: $2O_2^{\bullet-} + 2H_2O \rightarrow 2OH^- + H_2O_2 + O_2$ (Halliwell and Gutteridge, 1999)].

[c]$^{\bullet}OH$ was determined on untreated solid sample mixed with the $^{\bullet}OH$ assay reagents solution.

[d]Sample 1 was extracted in ACN_{alk}-CE solvent, where sample $Mg(ClO_4)_2$ was completely dissolved in this solvent (designated "ACN-solid solution").

[e]In samples 2 and 3, extraction with ACN_{alk}-CE solvent resulted in two fractions (after centrifugation), the clear supernatant (designated "ACN-extract") and an ACN-insoluble solid precipitate, which was extracted with ddH_2O (designated "ACN/H_2O-solid extract") in order to measure released H_2O_2.

[d,e]ACN_{alk}-CE-extracted nonradiolyzed $Mg(ClO_4)_2$ alone (the control of sample 1), and non-radiolyzed $Mg(ClO_4)_2$ mixed with the salt analogue (the control of sample 3) did not generate any H_2O_2, $O_2^{\bullet-}$, or $^{\bullet}OH$.

[f]This total H_2O_2 nmol value from sample 3 is the sum of the 1.0 nmol H_2O_2 from the 0.5 nmol $O_2^{\bullet-}$ (after dismutation) in the ACN extract, the 1.95 nmol H_2O_2 in the same extract, and the 0.63 nmol H_2O_2 in the ACN/H_2O-solid extract.

n/a = not available.

these species. This assay was developed by using KO_2 and was experimentally validated with MgO_2, CaO_2, and Na_2O_2 (Table 2), and NaClO and $NaClO_2$ (Table 3). The detailed methods used in these experiments are presented in the Supplementary Materials (available online at www.liebertonline.com/ast). In the present section, the assay principle and its validation experiments are briefly overviewed.

Assay principle and validation: The superoxide-peroxide assay is an extension of the Fe^{2+}-xylenol orange (FOX) assay (Grintzalis *et al.,* 2013; Georgiou *et al.,* 2015) for soil $O_2^{\bullet-}$. It measures sample $O_2^{\bullet-}$ (after dismutation to H_2O_2 and O_2) and sample H_2O_2 in separate assay steps following extraction in alkaline acetonitrile (ACN_{alk}) containing dicyclohexano-18-crown-6 ether (CE). After extraction, the ACN_{alk}-CE extract is split into two fractions, one for $O_2^{\bullet-}$ and the other for H_2O_2 determination. In the $O_2^{\bullet-}$ determination procedure, CAT is used to eliminate H_2O_2, and subsequently $O_2^{\bullet-}$ is dismutated using ddH_2O (at 50% ACN final concentration) and quantified as H_2O_2. Sample $O_2^{\bullet-}$ concentration is determined based on $O_2^{\bullet-}$ dismutation stoichiometry ($O_2^{\bullet-} + H_2O \rightarrow OH^- + \frac{1}{2}H_2O_2 + \frac{1}{2}O_2$). For H_2O_2 determination, CAT is not used, and $O_2^{\bullet-}$ is dismutated (at 50% ACN in water) to H_2O_2. Total H_2O_2 is determined, and then the concentration of sample H_2O_2 is determined by subtracting the measured quantity H_2O_2 from the quantity of H_2O_2 measured in the $O_2^{\bullet-}$ determination procedure.

The superoxide-peroxide assay was validated for the quantification of $O_2^{\bullet-}$ by using two different standard methods for $O_2^{\bullet-}$ determination. In the first method, a HE-based fluorometric assay (Georgiou *et al.,* 2015), $O_2^{\bullet-}$ (from reagent KO_2) was measured (at 1 m*M* HCl, 40 μM HE) in runs by using ACN (containing 0.2–1 m*M* CE) over a concentration range of 95–20% (at pH 7.0) with 99% ACN_{alk} as control. The second method, the superoxide dismutase–inhibited reduction of cytochrome *c* by $O_2^{\bullet-}$, was used to test the dismutation of $O_2^{\bullet-}$ (from reagent KO_2) in ACN over a concentration range up to 50%. The results of these tests were compared to the method developed for the present study. All three methods gave same results on the $O_2^{\bullet-}$ measurement in the tested 95–20% ACN solutions, and show that the dismutation of $O_2^{\bullet-}$ radical takes place below 80% ACN (Fig. 1a). Moreover, the tested incubation intervals with CAT (500 and 50 units) of the (respective 95–70% and 60–20% range) ACN $O_2^{\bullet-}$ solutions in the second method showed that $O_2^{\bullet-}$ was stable even at the limit of the 80% ACN concentration and for the 10 min incubation period used in the superoxide-peroxide assay.

The effect of ACN-CE concentration on the superoxide-peroxide assay standard curve (0–2 μM H_2O_2) was tested to determine the optimum assay sensitivity (*i.e.,* the maximum standard curve slope for different ACN_{alk}-CE extract concentrations). The slope is an exponential function of % ACN (Fig. 1b), with CE concentration not affecting the slope (tested to 8 m*M*). Based on the exponential function, the maximum slope to sample dilution factor ratio (0.13/2) is

Table 2. H_2O_2 Generation by Metal Peroxide Commercial Analogues

ROS formed		H_2O_2[a]		
Samples[b]	*Extraction treatment*	*Unheated*	*Heated*	*Fold*[a]
MgO_2	i. ACN-extract[c]	0.29[d] (0.029)	0.19[d] (0.019)	1.5↓
	ii. ACN/H_2O-solid extract[c]	1.41[d] (0.14)	0.56[d] (0.056)	2.5↓
CaO_2	i. ACN-extract[c]	1.59[e] (0.16)	0.72[e] (0.072)	2.2↓
	ii. ACN/H_2O-solid extract[c]	25.5[e]	25.5[e]	1[e]
Na_2O_2	i. ACN-extract[c]	0.64[f] (0.064)	0.36[f] (0.036)	1.8↓
	ii. ACN/H_2O-solid extract[c]	185[f]	185[f]	1[f]

[a]Concentrations of H_2O_2 are expressed as nmol (in 1 mL extract) per 1 μmol of indicated sample. The concentration values in parentheses are in mol % expressed in, *e.g.,* nmol H_2O_2 produced from 100 nmol MgO_2/CaO_2/Na_2O_2. Fold changes of heated over unheated sample are shown with upward (increase) and downward (decrease) arrows.

[b]Sample quantities tested: MgO_2 (1.3, 2.6, 5.2, 10.4 mg), CaO_2 (0.65, 1.63, 3.25, 13.0 mg), and Na_2O_2 (0.95, 1.9 mg).

[c]Samples were extracted with 1 mL ACN_{alk}-CE solvent and resulted in two fractions (after centrifugation): a clear supernatant (designated ''ACN-extract'') and an ACN-insoluble solid precipitate, which was extracted with 1 mL ddH_2O (designated ''ACN/H_2O-solid extract'').

[d]H_2O_2 nmol values for MgO_2 extracted in 1 mL ACN_{alk}-CE solvent (in ACN extract) were constant (averaging 5.1 and 3.4 nmol for the unheated and the heated sample, respectively) for all tested mg quantities, suggesting maximum solubility levels, the difference of which between unheated and heated sample may be due to the solubility effect of possible heat-generated by-products. The corresponding values for the ACN/H_2O-solid extract were not proportional at >1 mg MgO_2 due to H_2O_2 instability at the high alkaline pH in the extract [created by $Mg(OH)_2$ formation via the hydrolysis reaction: $MgO_2 + 2H_2O \rightarrow Mg(OH)_2 + H_2O_2$].

[e]H_2O_2 nmol values for CaO_2 extracted in 1 mL ACN_{alk}-CE solvent (in ACN extract) were proportional for the unheated sample up to 1.5 mg (above which they reached a maximum solubility of 40 nmol mL^{-1}) and heated at 1.5 mg. The nmol in the ACN/H_2O-solid extract may not be equal at the reported value for 0.65 mg unheated/heated CaO_2, as at this mg quantity and above the hydrolysis product H_2O_2 may be quite unstable due to the high alkaline pH (>10) of the extract [because of $Ca(OH)_2$ formation by hydrolysis reaction: $CaO_2 + 2H_2O \rightarrow Ca(OH)_2 + H_2O_2$].

[f]H_2O_2 nmol values for both unheated and heated Na_2O_2 extracted in 1 mL ACN_{alk}-CE solvent (in ACN extract) and in the ACN/H_2O-solid extract were proportional for the tested quantities. However, the H_2O_2 nmol in the ACN/H_2O-solid extract may not be equal at the reported value for 0.95 mg unheated/heated Na_2O_2 due to the instability of H_2O_2 due to the quite high alkaline pH increase (>12.5) observed in the extract [because of NaOH formation by the hydrolysis reaction: $Na_2O_2 + 2H_2O \rightarrow 2NaOH + H_2O_2$].

TABLE 3. H_2O_2 GENERATION BY ClO^- AND ClO_2^-

ROS formed		H_2O_2[a]	
Samples	*Extraction treatment*	*Unheated*	*Heated*
$NaClO_2$[b]	i. ACN-extract[c]	9.0[d] (0.9)	9.0[d] (0.9)
	ii. ACN/H_2O-solid extract[c]	425[d] (43)	425[d] (43)
NaClO[b]			
Dry NaClO-unheated[f]/Dry NaClO-heated[g]	i. ACN-extract[c]	17.4[e] (1.7)	18.3[f] (1.8)
	ii. ACN/H_2O-solid extract[c]	14.8[e] (1.5)	16.0[f] (1.6)
		..... sum = 32.2 (3.2)	..... sum = 34.3 (3.4)
Controls:			
Liquid NaClO-unheated	NE[c]	84.0 (8.4)	—
Dry NaClO-unheated[f]	NE[c]	83.7[e] (8.4)	—
Dry NaClO-heated[g]	NE[c]	—	83.3[f] (8.3)

[a]Concentration values of H_2O_2 are expressed in nmol (in 1 mL extract) per 1 μmol of indicated sample. The concentration values in parentheses are in mol %, expressed as, *e.g.,* nmol H_2O_2 produced from 100 nmol NaClO/$NaClO_2$.

[b]Tested quantities: $NaClO_2$ (10–200 μmol). NaClO was tested as ([b]) solidified in fumed silica (see preparation and heat-treatment recoveries in Materials and Methods), (i) dry NaClO-unheated (190 nmol), and dry NaClO-heated (30 nmol recovered from 820 nmol initially contained in 90 mg dry NaClO-heated), and (ii) liquid NaClO-unheated (1 nmol from a 7.6 m*M* NaClO stock).

[c]Samples were extracted with 1 mL ACN_{alk}-CE solvent, and after centrifugation they resulted in two fractions: a clear supernatant (designated ''ACN-extract'') and an ACN-insoluble solid precipitate, which was further extracted with 1 mL ddH_2O (designated ''ACN/H_2O-solid extract''). NaClO controls were not extracted (NE) in ACN; they were mixed and diluted in ddH_2O before being assayed for H_2O_2 and $O_2^{\bullet-}$ production.

[d]H_2O_2 nmol values for $NaClO_2$ in ACN extract (*i.e.,* extracted in 1 mL ACN_{alk}-CE solvent) were constant (averaging 100 nmol per 1 mg $NaClO_2$ for both unheated and heated sample), which suggests maximum solubility levels attained, while the corresponding nmol values for the ACN/H_2O-solid extract were proportional to the tested mg quantities of $NaClO_2$.

[e]Values for dry NaClO-unheated sample.

[f]Values for dry NaClO-heated sample.

achieved at 50%. (For example, at 20% the slope to sample dilution factor is 0.17/5. Therefore, the optimum ACN concentration was chosen at 50% for performing the assay.)

The CAT activity in various concentrations of ACN was examined to verify its efficiency to decompose H_2O_2 over a range of incubation intervals (up to 10 min) and H_2O_2 concentrations (up to 2 m*M*). The results of this test verified that co-extracted O_2^{2-} is removed from sample fraction 1, without loss of $O_2^{\bullet-}$ (Fig. $1c_1$). Since CAT heme iron may interfere with the assay, the optimum CAT units for the decomposition of H_2O_2 (at assay final 50% ACN, containing 10 m*M* phosphate buffer, pH 7.5) were determined. As control, CAT interference (at 50% ACN) was measured (as absorbance at 560 nm) in the absence of H_2O_2. Based on these results to minimize its heme iron interference, a maximum 30 units CAT (per milliliter assay mixture) was used in the assay (Fig. $1c_2$).

Assay sensitivity was determined to be ~70 pmol $O_2^{\bullet-}$ and 35 pmol H_2O_2 co-extracted in 100% ACN (and determined at 50% ACN) and 14 pmol H_2O_2 when the assay is used only for H_2O_2 determination in H_2O extracts of solid samples. The details of assay protocol used for peroxide and superoxide determinations are given in the Supplementary Materials.

2.4. Hydroxyl radical assay

Quantification of $^{\bullet}OH$ is performed by a modification of a previous method (Georgiou *et al.,* 2015). The method is based on the specific reaction of $^{\bullet}OH$ with TPA in Na-borate buffer, pH 9, and the formation of the fluorescent product 2-hydroxy terephthalic acid (2HTPA) measured at 423 nm (311 nm excitation). Net peak emission fluorescence is obtained against the controls Na-borate-TPA and Na-borate-sample (at the highest tested concentration). Identification of $^{\bullet}OH$ is performed by the inhibition of 2HTPA formation with the presence in a Na-borate-TPA assay solution of 100 m*M* DMSO, a well-known scavenger of $^{\bullet}OH$. The net fluorescence units (FU) of 2HTPA are converted to nanomoles of $^{\bullet}OH$ by a standard curve (see the Supplementary Materials).

2.5. Effect of ClO_2^- and ClO^- on $^{\bullet}OH$ standard curve

Since production levels of $^{\bullet}OH$ are assessed indirectly by the production levels of 2HTPA, its quantification by the $^{\bullet}OH$ assay may be underestimated due to its fluorescence quenching by the presence of possible oxidants such as ClO^- and ClO_2^-. These are well-known products of the radiolysis of metal perchlorate (Prince and Johnson, 1965; Paviet-Hartmann *et al.,* 2001; Quinn *et al.,* 2013); thus their

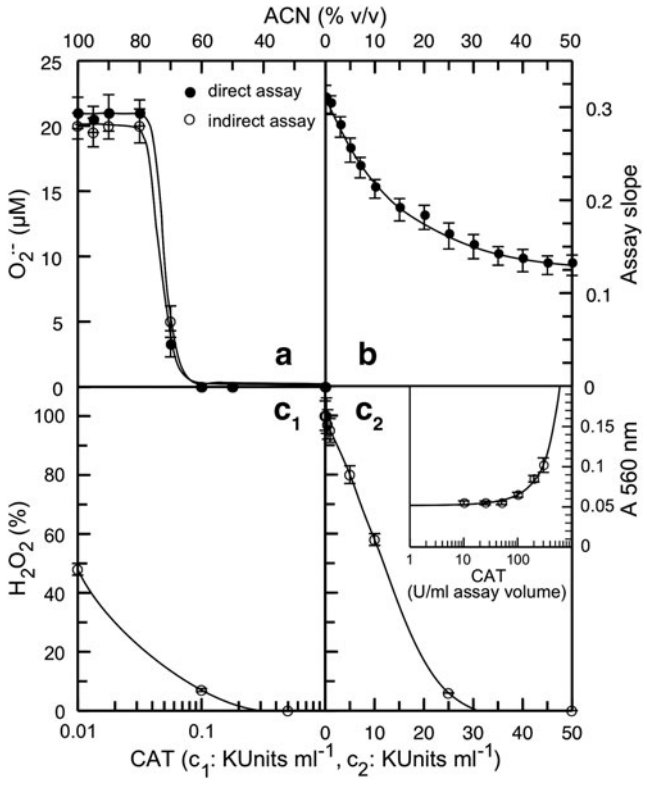

FIG. 1. Parameters of the inorganic origin $O_2^{\bullet-}/H_2O_2$ assay: (**a**) Dismutation of $O_2^{\bullet-}$ (21 μM) as a function of ACN concentration, measured directly (as $O_2^{\bullet-}$) and indirectly as H_2O_2 (the product of $O_2^{\bullet-}$ dismutation) by the HE-based fluorometric (direct) in comparison to the present assay (indirect). (**b**) H_2O_2-based slope of the assay, expressed as absorbance (at 560 nm) per 1 μM H_2O_2, as a function of ACN concentration. (**c_1**) Decomposition of H_2O_2 (100% = 1 mM) by CAT (from stock 20 KU/mL) in 95% ACN (in 15 mM phosphate buffer, pH 7.5, and 0–5 mM CE) after incubation for 10 min. The assay was tested in 500-fold dilutions of the incubation mixture (at ~0% ACN). (**c_2**) Decomposition of H_2O_2 (100% = 100 μM) by CAT in 50% ACN (in 10 mM phosphate buffer, pH 7.5) after incubation for 5 min. The assay was tested in 50-fold dilutions of the incubation mixture (at ~50% ACN). Inset shows CAT interference at 50% ACN in the assay as measured by the assay absorbance at 560 nm. Error bars designate standard error.

possible presence in radiolyzed $Mg(ClO_4)_2$ alone/mixed with the Mars Phoenix site salt analogue may underestimate 2HTPA (thus $^{\bullet}OH$) production levels. The same 2HTPA oxidation issue will arise when assessing photolyzed ClO^- and ClO_2^- as potential sources of $^{\bullet}OH$. Another consideration arises from the fact that the actual molar ratio 2HTPA/$^{\bullet}OH$ (the theoretical is 1:1) must be determined under the conditions of the $^{\bullet}OH$ assay in order to estimate accurately the production levels of $^{\bullet}OH$. This is established by the construction of a standard curve of 2HTPA FU versus $^{\bullet}OH$ under the same conditions for the $^{\bullet}OH$ assay. Details of these tests are given in the Supplementary Materials.

2.6. NaClO solidification and heating: recovery

For investigating ClO^- as generator of H_2O_2 and $^{\bullet}OH$ (Table 3 and Fig. 4, respectively) in the solid form, as produced in radiolyzed $Mg(ClO_4)_2$, ''solid'' ClO^- was formed by drying (evaporating) NaClO mixed with fumed silica. Recovery was determined after solidification and heating at 160°C for 3 h. It should be noted that NaClO solution upon drying produces—stable at ~20°C to ~50°C—the hydrated forms $NaClO \cdot 5H_2O$ and $NaClO \cdot 2.5H_2O$ (Elsenousy and Chevrier, 2014). Details of these tests are given in the Supplementary Materials.

2.7. Products from UVC-photolyzed ClO^- and ClO_2^-

ClO^- and ClO_2^- were photolyzed by UVC in order to study, under simulated martian topsoil UV exposure conditions, their conversion to Cl-based products, which could act as photolysis-induced generators of $^{\bullet}OH$ (see subsequent experiment and Fig. 4). Experimental details are given in the Supplementary Materials.

2.8. Generation of $^{\bullet}OH$ by radiolyzed $Mg(ClO_4)_2$ and the Mars Phoenix site salt analogue, and by metal peroxide analogues

$Mg(ClO_4)_2$, the Mars Phoenix salt analogue (with and without perchlorate; radiolyzed and nonradiolyzed), and commercial MgO_2, CaO_2, and Na_2O_2 were tested for $^{\bullet}OH$ production (Tables 1 and 2), following the procedure of the aforementioned $^{\bullet}OH$ assay.

2.9. $^{\bullet}OH$ generation by UVA photolysis of ClO^- and ClO_2^-

Due to the very fast UVC photolysis of NaClO and $NaClO_2$ (Fig. 3), ClO^- and ClO_2^- were investigated as potential sources of $^{\bullet}OH$ under time-controlled UVA exposure (Fig. 4). Experimental details are provided in the Supplementary Materials.

2.10. Statistical analysis

All data are reported as mean ± standard error of at least three independent experiments and were analyzed with the SPSS statistical package (SPSS Inc., 2001, Release 11.0.0, USA). Whenever appropriate, the significance was determined for Student's unpaired t test or ANOVA. A value of $P < 0.05$ was considered to be significant.

3. Results

3.1. Superoxide and peroxide production by radiolysis of $Mg(ClO_4)_2$ and Phoenix salt analogue

Generation of $O_2^{\bullet-}$ and H_2O_2 by radiolysis of $Mg(ClO_4)_2$ and the Phoenix salt analogues is shown in Table 1. $O_2^{\bullet-}$ was detected only in the perchlorate-containing salt analogue at 1 nmol per 80 mg of analog sample (80 mg of salt sample corresponds to the measured salt content in 1 cc of regolith at the Phoenix site and contains 58.3 μmol ClO_4^-). The same sample produced ~2 nmol of H_2O_2. No $O_2^{\bullet-}$ and 3.3-fold less H_2O_2 were measured in the sample after heating at 160°C for 3 h. H_2O_2 was also produced, at a level of ~6 nmol per 58.3 μmol ClO_4^-, by radiolyzing the pure $Mg(ClO_4)_2$, and was reduced by 61-fold by heating the sample. No H_2O_2 or $O_2^{\bullet-}$ was measured in the radiolyzed

salt mixture that did not contain perchlorate. In addition, no H_2O_2 or $O_2^{\bullet-}$ production was measured in any of the three sample types if they were not irradiated (control samples).

Control experiments were run on metal peroxides MgO_2, CaO_2, and Na_2O_2 to verify the ability of the assay to quantify $O_2^{\bullet-}$ and H_2O_2 and to determine whether they may be sources of H_2O_2 via hydrolysis (Table 2) if they are generated during radiolysis of $Mg(ClO_4)_2$ and/or the Phoenix site salt analogue (with and without perchlorate). Additionally, NaClO and $NaClO_2$ were tested using the assay to determine whether they generate H_2O_2 (Table 3) because hypochlorite (ClO^-) and chlorite (ClO_2^-) are produced by radiolyzed perchlorate (Prince and Johnson, 1965; Paviet-Hartmann *et al.,* 2001; Quinn *et al.,* 2013).

H_2O_2 was measured in MgO_2 and Na_2O_2 (unheated) ACN_{alk}-CE extracts at levels of 0.029 and 0.064 mol %, respectively, which are comparable to the levels measured with radiolyzed $Mg(ClO_4)_2$ (0.011 mol %). H_2O_2 levels measured in CaO_2 (unheated) ACN_{alk}-CE extracts were 2.5- and 5.5-fold higher than those measured for Na_2O_2 and MgO_2, respectively. H_2O_2 generation by MgO_2, CaO_2, and Na_2O_2 was decreased by heating them (at 160°C for 3 h) by 1.8-fold on average, while heating decreased H_2O_2 generation by radiolyzed $Mg(ClO_4)_2$ by 61-fold (Tables 1 and 2). The ACN-insoluble fractions of unheated and heated MgO_2, CaO_2, and Na_2O_2 produced much higher levels of H_2O_2 upon solubilization in ddH_2O than the soluble fractions, with ddH_2O-dissolved MgO_2 producing the lowest levels (0.14 and 0.056 mol % unheated and heated, respectively; Table 2).

On the other hand, the ACN_{alk}-CE-extracted unheated and heated (at 160°C for 3 h) controls $NaClO_2$ and NaClO produced ~80- and ~150-fold higher H_2O_2 concentration levels (0.9 and 1.7% mol) than ACN_{alk}-CE-extracted unheated radiolyzed $Mg(ClO_4)_2$, respectively (Tables 3 and 1). This is consistent with the fact that the levels of ClO_2^- and ClO^- in the radiolyzed $Mg(ClO_4)_2$ are only a small mole fraction of the sample. The concentration (% mol) of H_2O_2 as the sum of the ACN- and ACN/H_2O-solid extract fractions for the unheated and heated NaClO (~3) is almost 40% of that for the non-ACN-fractionated ''liquid unheated,'' ''dry unheated,'' or ''dry heated'' controls (Table 3), which suggests a less than 100% recovery during the ACN fractionation procedure.

The concentration of H_2O_2 produced by heating NaClO was determined in comparison to the fraction that was retained after heating. NaClO was solidified in fumed silica, and its recovery was measured after heating to test it as a solid-state generator of $^{\bullet}OH$ upon UV exposure. Liquid NaClO was solidified in fumed silica by vacuum evaporation as described in Materials and Methods and in Fig. $4a_1$. Recovery of ClO^- by the solidification process (water removal at <50°C) was 55.6%, while after heating (for 3 h at 160°C) recovery was ~3%. $NaClO_2$ was heat stable.

3.2. $^{\bullet}OH$ generated by radiolyzed $Mg(ClO_4)_2$ and Mars Phoenix site salt analogue: $^{\bullet}OH$ assay and control experiments

Radiolyzed $Mg(ClO_4)_2$ produced ~1 nmol $^{\bullet}OH$ (0.0017 mol %) per 58.3 μmol ClO_4^- when unheated. Interestingly, ~7-fold higher levels were measured in the radiolyzed samples after they were heated. More importantly, both unheated complete and incomplete salt analogues produced a ~150-fold higher concentration of $^{\bullet}OH$ (149 and 147 nmol per 80 and 73.5 mg, respectively, corresponding to 1 cc martian soil). $^{\bullet}OH$ production by the complete and the incomplete analogues decreased by an average of ~2.5-fold when heated (Table 1). However, $^{\bullet}OH$ production by the heated complete salt analogue (75 nmol; Table 1) was 33% higher than by the heated incomplete. The nonradiolyzed controls of all these samples did not produce $^{\bullet}OH$.

Hypochlorite (ClO^-) and chlorite (ClO_2^-) were investigated as possible sources of $^{\bullet}OH$ in radiolyzed $Mg(ClO_4)_2$ and Mars Phoenix site salt analogue because they have been identified in the main radiolysis products of radiolyzed metal perchlorate [and $Mg(ClO_4)_2$] (Prince and Johnson, 1965). These were studied by using their corresponding analogues NaClO and $NaClO_2$ in an extensive array of experiments designed to test the following: (i) whether NaClO and $NaClO_2$ oxidize the fluorescent 2HTPA (Fig. 2) by which $^{\bullet}OH$ is indirectly quantified, resulting in underestimation of $^{\bullet}OH$ concentration; (ii) UV photolysis of NaClO and $NaClO_2$ with the intent to study them as possible sources of Cl-based byproducts (Fig. 3) under simulated martian UVC exposure

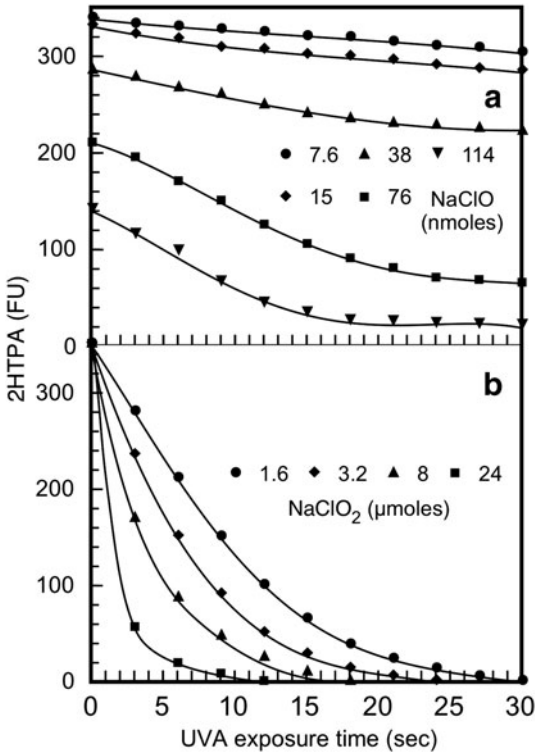

FIG. 2. Effect of ClO^- and ClO_2^- on the $^{\bullet}OH$ assay standard curve: The effect of NaClO (**a**) and $NaClO_2$ (**b**) concentrations (nanomolar and micromolar, respectively) was studied on the fluorescence quenching of 2HTPA (the specific product of the reaction of $^{\bullet}OH$ with its specific trap TPA). 2HTPA FU were studied as a function of (i) the concentration of NaClO and $NaClO_2$ [since ClO^- and ClO_2^- are generated by the radiolysis of perchlorate (Prince and Johnson, 1965; Paviet-Hartmann *et al.,* 2001) and by UVC photolysis of ClO_2^- shown in Fig. 3], and (ii) their time exposure to UVA (serving also as control to their study as generators of $^{\bullet}OH$; see Fig. 4).

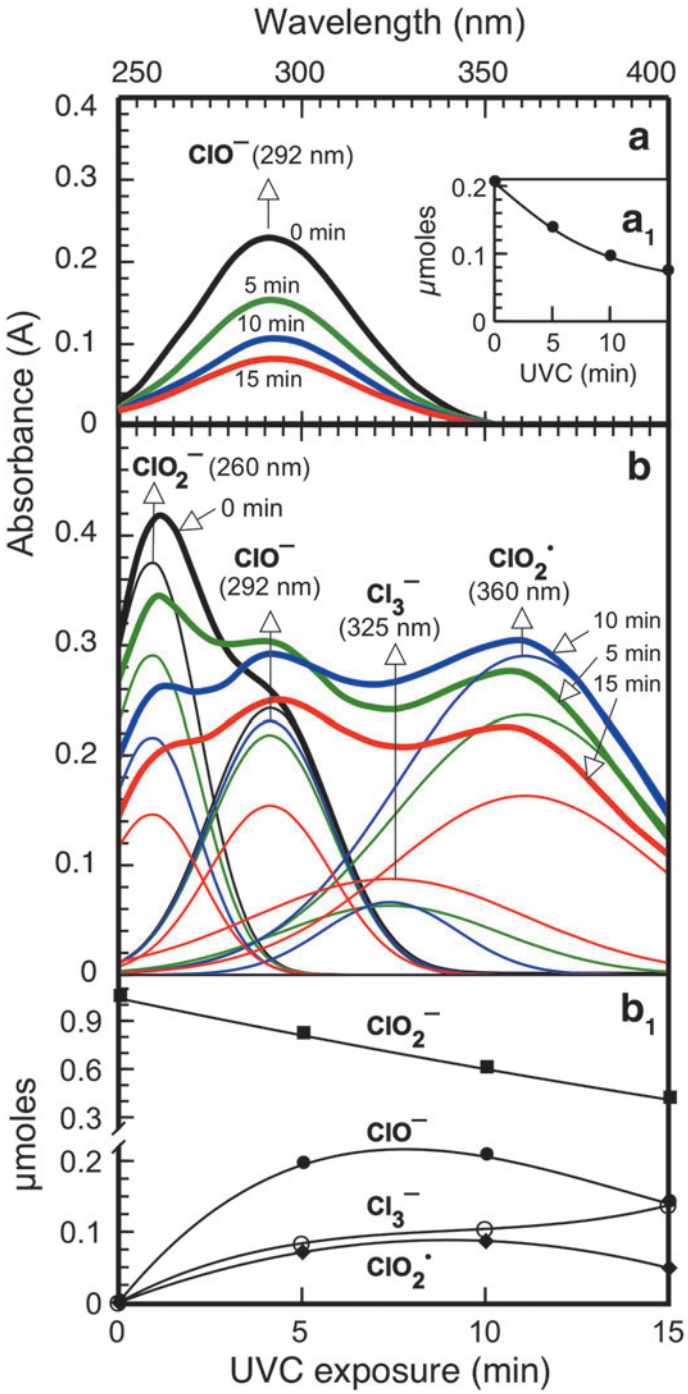

FIG. 3. UVC photolysis products of NaClO and $NaClO_2$: (**a**) Spectra of ~0.2 μmol NaClO (in 0.3 mL solution); inset (a_1) presents the peak absorbance change of NaClO at 292 nm versus UVC exposure time. (**b**) Spectra of ~1.0 μmol $NaClO_2$ (in 0.3 mL solution) at zero time exposure. Actually, the zero time spectra of $NaClO_2$ should have only one maximum absorbance peak at 260 nm. However, they appear to contain an extra peak at 292 nm (belonging to ClO^- as identified by spectrum deconvolution), most likely the outcome of exposing $NaClO_2$ to the light source of the spectrophotometer during 250–400 nm spectrum recording [giving an apparent molar ratio 4.8 $NaClO_2$/NaClO, based on their molar absorption coefficients 108 and 335 M^{-1}, respectively (Paviet-Hartmann *et al.,* 2001)]. However, this question is resolved in the analysis of the spectra obtained after exposing $NaClO_2$ to UVC for 5, 10, and 15 min. The resulted spectra are composed of overlapping peaks, which after being resolved (see corresponding thinner lines) by a spectral peak deconvolution software (see Materials and Methods) were identified to belong to ClO^- (292 nm), Cl_3^- (325 nm), and $ClO_2^{\bullet}$ (360 nm) (Paviet-Hartmann *et al.,* 2001). Panel (**b_1**) presents the micromolar change (in 0.3 mL solution) of these peaks as a function of UVC exposure time. The curve fit of the 290 nm peak absorbance value changes for ClO^- during 5, 10, and 15 min UVC exposure shows that its absorbance value at zero minutes' exposure is zero. The same conclusion is derived from the oxidation of 2HTPA by $NaClO_2$, where the curves of 2HTPA fluorescence quenching as function of different concentrations of $NaClO_2$ at different UVC exposure times converge to the initial FU of 2HTPA at zero time exposure (Fig. 2b). This convergence would not have happened if $NaClO_2$ and NaClO coexisted at a molar ratio 4.8, as NaClO would have been present at high nanomolar concentration that would have oxidized 2HTPA (decreased its initial FU) even at zero-time UVC exposure (Fig. 2a).

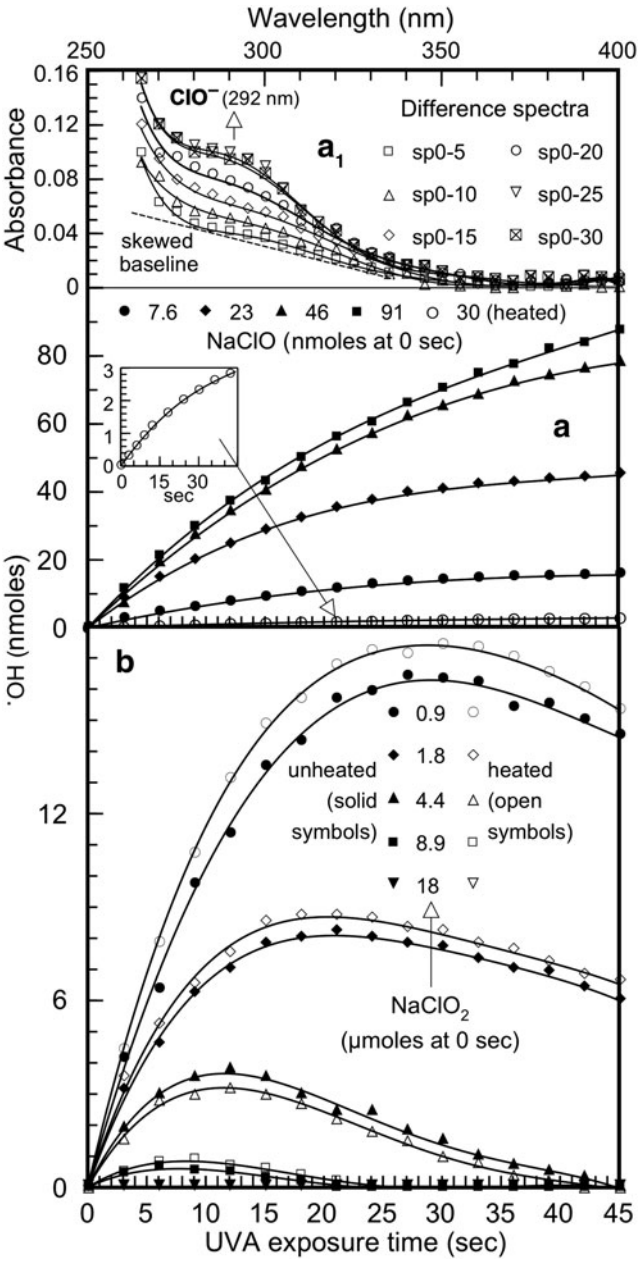

FIG. 4. Hydroxyl radical generation by UVA photolysis of ClO^- and ClO_2^-: $^{\bullet}OH$ is shown to be generated by their commercial analogues NaClO (**a**) and $NaClO_2$ (**b**), respectively (unheated, solid symbols, and heated, open symbols), at different concentrations as function to UVA exposure time. Inset in (a) is a magnification of the concentration rate curve of $^{\bullet}OH$ produced by heated NaClO, the solidification of which and its heat recovery (determined by difference spectra shown in $\mathbf{a_1}$) are described in Materials and Methods.

conditions; and (iii) subsequently NaClO and $NaClO_2$ as generators of $^{\bullet}OH$ by a more time-controlled UV exposure (using the less energetic UVA) (Fig. 4).

(i) It was found that both NaClO and $NaClO_2$ oxidize 2HTPA. At 0 s UVA exposure, 7.5 and 38 nmol NaClO oxidize 2HTPA moderately. Higher concentrations oxidized to a much greater degree, resulting in an underestimation of $^{\bullet}OH$ concentration by the employed assay. For example, 114 nmol NaClO decreased the initial 350 FU of 2HTPA to 150 FU (Fig. 2a). On the other hand, $NaClO_2$ did not oxidize 2HTPA even at 1000-fold higher quantities (1.6 to 24 μmol), and is shown by the extrapolation of the UVA exposure 2HTPA FU curves, which cross the *y* axis at the initial 350 FU (Fig. 2b). However, the oxidative destruction of the HTPA FU by $NaClO_2$ is evident as a function of UVA photolysis time. This is possibly due to the UVA-induced release of NaClO by photolyzed $NaClO_2$ as is seen in UVC photolysis (Fig. 3b), and the concomitant production of $^{\bullet}OH$ followed by its 2HTPA oxidizing effect (Fig. 4b and unpublished experimental observation). This is also supported by the increasing destruction of the initial FU of 2HTPA (at 0 s UVA exposure) by NaClO, as the concentration of the latter increases from 7.6 to 114 nmol (Fig. 2a). On the other hand, the destruction of 2HTPA FU by the UVA photolysis of NaClO becomes more profound at high NaClO concentrations (Fig. 2a) and is possibly due to the oxidation of 2HTPA by $^{\bullet}OH$ (as it is shown to be produced at higher rates; Fig. 4a).

(ii) Possible UVC photolysis products of NaClO and $NaClO_2$ were investigated spectrally under simulated martian UV exposure conditions (Fig. 3). It was found that NaClO decreased in concentration without producing any spectrally identified Cl-based species (Fig. 3a, $3a_1$). On the other hand, $NaClO_2$ was photolyzed to the Cl-based oxidants ClO^- (292 nm), Cl_3^- (325 nm), and $ClO_2^{\bullet}$ (360 nm). The concentration changes of these species versus exposure time were determined by their known molar extinction coefficients (Paviet-Hartmann *et al.,* 2001). The individual spectral peaks were resolved by the spectral peak deconvolution of the composite spectra, obtained at various UVC exposure-time intervals (5, 10, 15 min).

(iii) After investigations i and ii as described above, NaClO and $NaClO_2$ were then tested for $^{\bullet}OH$ generation under simulated martian soil UV exposure conditions. The aim was to uncover a possible mechanism of $^{\bullet}OH$ generation based on the UVA photolysis of the radiolysis products of $Mg(ClO_4)_2$ (Fig. 4), which would complement its radiolysis mechanism for $^{\bullet}OH$ production (shown in Table 1). Unheated and heated NaClO (*i.e.,* solidified) and $NaClO_2$ both produced $^{\bullet}OH$ only upon photolysis by UVA (311 nm) at an increasing rate as a hyperbolic function of exposure time, which became horizontal to the *x* axis for NaClO at low concentrations (Fig. 4a). The fact that 30 nmol of heated NaClO produced $^{\bullet}OH$ at a 25-fold lower initial concentration rate than the average concentration of the 23 and 46 nmol unheated NaClO may be attributed to the fact that the heated sample contained NaCl in an approximate concentration 4 *M* in the $^{\bullet}OH$ assay 0.3 mL solution (for explanation, see the Supplementary Materials). Such high Cl^- anion concentration is known to scavenge $^{\bullet}OH$ (Liao *et al.,* 2001). On the other hand, the rate curves for $NaClO_2$ peaked and then declined over extended time exposure. This could be due to the possible production of the photolysis product NaClO (Fig. 3a), which oxidizes 2HTPA (Fig. 2).

4. Discussion

4.1. Methodological justification of the inorganic-origin superoxide/peroxide assay

Radiolyzed $Mg(ClO_4)_2$ and complete and incomplete Mars Phoenix site salt analogue were analyzed for generation of H_2O_2, $O_2^{\bullet-}$, and $^{\bullet}OH$ (Table 1) and compared (i) to peroxide

analogues based on the metal ions present the salt analogues and (ii) known perchlorate radiolysis product analogues. The assay used for analysis extracts both $O_2^{\bullet-}$ and H_2O_2 from samples in an anhydrous alkaline ACN_{alk}-CE (or ACN_{alk}) solvent, which is then split into two fractions. Each fraction is then subjected to different reaction treatments in order to identify and quantify stable $O_2^{\bullet-}$ and H_2O_2. The first fraction contains $O_2^{\bullet-}$ that may be present in the sample as metal superoxides (extracted by metal cation dissociation using CE, and at the same time stabilized in the ACN_{alk} solvent) or trapped inside mineral lattices, which is quantified as H_2O_2 upon dismutation. In the same fraction, the assay also determines sample peroxides (free or as metal peroxides). Although H_2O_2 is normally unstable at high alkaline pH, it remains stable at the ACN_{alk}-CE solvent's mild alkaline pH ($\sim$8) (Georgiou *et al.,* 2016). Subsequent CAT treatment steps discriminate the H_2O_2 fraction attributed to $O_2^{\bullet-}$ from that attributed to peroxides. The second ACN_{alk}-CE solvent fraction also contains ACN_{alk}-CE-soluble metal peroxides and superoxides, which are detected as H_2O_2 after hydrolysis and dismutation (in H_2O), respectively. The ACN_{alk}-CE fractionation step of the present assay proved to be advantageous for the $Mg(ClO_4)_2$ component because it is completely solubilized in the ACN solvent, which is crucial for the identification of the possible sources of $O_2^{\bullet-}$ and H_2O_2.

4.2. Generation of H_2O_2 and $O_2^{\bullet-}$ in radiolyzed $Mg(ClO_4)_2$ and the Mars Phoenix salt analogue

We find that the amount of H_2O_2 measured in radiolyzed $Mg(ClO_4)_2$ extracted with ACN_{alk}-CE solvent is 3.3-fold higher (0.011%) compared to the ACN-extracted complete salt analogue (0.0033% H_2O_2). This suggests that in the salt analogue that contained $Mg(ClO_4)_2$, the $O_2^{\bullet-}$ that forms may be stabilized by the Na^+, K^+, and Ca^{2+} that are present in the analogue. Supporting evidence for this $O_2^{\bullet-}$ stabilization pathway comes from the low levels of H_2O_2 that are detected in the H_2O extracts of the complete and the incomplete salt analogues (0.63 and 0.57 nmol, respectively) compared to $Mg(ClO_4)_2$ alone (6.27 nmol). It should be noted that no H_2O_2 was detected in the ACN extract of the radiolyzed salt analogue that did not contain perchlorate. This suggests that, if metal peroxides and/or superoxides originate from oxygen that may be released by the radiolysis of ClO_4^- or SO_4^{2-} in the analogue, they are not associated with the analogue ions Na^+, Ca^{2+}, and Mg^{2+} because MgO_2, CaO_2, and Na_2O_2 were shown to be partly soluble in ACN (Table 2). The CO_3^{2-} component of the complete salt analogue may not play a role in the generation of metal peroxides and superoxides, since radiolysis of CO_3^{2-} has been associated with the formation of the carbonate radical ($^{\bullet}CO_3^-$) after CO_3^{2-} (or HCO_3^-) reaction with $^{\bullet}OH$ radicals (Haygarth *et al.,* 2010). On the other hand, H_2O_2 detected in the ACN extract of radiolyzed $Mg(ClO_4)_2$ could have resulted from the hydrolysis of MgO_2 due to the fact that its concentration also decreases upon heating (Table 2).

H_2O_2 cannot be generated directly from irradiated $Mg(ClO_4)_2$ simply because it lacks protons, although, if present, trace water could be a source of protons. However, H_2O_2 is produced during aqueous radiolysis of perchlorate (Konstantatos and Katakis, 1967), most likely from the dismutation of free $O_2^{\bullet-}$ and not through the hydrolysis of metal peroxides, because they (*e.g.,* MgO_2) do not form under aqueous conditions without preexistence of H_2O_2. H_2O_2 produced by radiolyzed $Mg(ClO_4)_2$ and the complete salt analogue may not have derived solely from the radiolysis products ClO_2^- and ClO^-, because controls $NaClO_2$ and NaClO produce $\sim$80- and $\sim$150-fold higher concentration levels of ACN_{alk}-CE-extracted H_2O_2, respectively, than unheated radiolyzed $Mg(ClO_4)_2$ (Table 3). On the other hand, the high levels of H_2O_2 produced by control NaClO as compared to those produced by radiolyzed $Mg(ClO_4)_2$ suggest that the minor fraction of the initial ClO^- that survived heating in radiolyzed $Mg(ClO_4)_2$ may explain the low levels of H_2O_2. Assuming that radiolyzed $Mg(ClO_4)_2$ produces ClO^- at same concentration as $Ca(ClO_4)_2$, which is a reasonable assumption given they have the same $G°$ value for ClO^- (0.03) (Prince and Johnson, 1965; Quinn *et al.,* 2013), the ClO^- in radiolyzed $Mg(ClO_4)_2$ that survived heating corresponds to 0.43 nmol. Based on the 1.7 mol % H_2O_2 produced by NaClO (Table 3), 0.43 nmol of ClO^- would be expected to produce 0.007 nmol H_2O_2, which is 14-fold lower than the experimentally measured value (0.1 nmol; Table 1). This difference in H_2O_2 production by radiolyzed $Mg(ClO_4)_2$ may be attributed to contribution by ClO_2^-, which is thermally stable. Given that the $Mg(ClO_4)_2$ $G°$ value for ClO_2^- production is 0.14 (Prince and Johnson, 1965), this would correspond to the production of $\sim$80 nmol ClO_2^- in the analogue; and considering the production of 9 nmol H_2O_2 per 1 μmol $NaClO_2$ (Table 3), the assumed 80 nmol ClO_2^- in heated radiolyzed $Mg(ClO_4)_2$ will produce $\sim$0.7 nmol H_2O_2, which is 7-fold higher than the experimentally measured value (0.1 nmol; Table 1).

Considering that 6.27 nmol H_2O_2 was produced by 6.5 mg radiolyzed $Mg(ClO_4)_2$, the actual 82 mg sample that was dissolved in 1.6 mL ACN_{alk}-CE to determine experimentally this value corresponds to 50 μM H_2O_2. On the other hand, the maximum concentration of commercial MgO_2 dissolved in ACN_{alk}-CE was 5.6 μM (data not shown); thus, the same concentration of H_2O_2 would have been produced from its hydrolysis reaction [$MgO_2 + 2H_2O \rightarrow Mg(OH)_2 + H_2O_2$]. The $\sim$9-fold higher concentration of H_2O_2 being produced by radiolyzed $Mg(ClO_4)_2$ may suggest the following: (i) either the radiolysis-generated MgO_2 is more readily dissolved if present in the crystal lattice of radiolyzed $Mg(ClO_4)_2$ (which was found to be readily dissolved in ACN) or (ii) H_2O_2 comes from a Mg-superoxide form such as $Mg(O_2)_2$ [its crystal structure has been identified (Bakulina *et al.,* 1970)], which may also be equally ACN soluble, or (iii) both.

It has been suggested that radiolyzed ClO_4^- decomposes mainly to chlorate ions (ClO_3^-) and O atoms either as aqueous solution (Katakis and Allen, 1964) or in solid form (Prince and Johnson, 1965). During the radiolysis of ClO_4^-, production of ClO_3^- and ClO_2^- appears to involve oxidation of hypochlorous acid (HOCl) or chlorous acid ($HClO_2$) via direct electron transfer, followed by reaction of the resulting chlorine monoxide ($ClO^{\bullet}$) or chloroperoxy radical ($ClOO^{\bullet}$) with $^{\bullet}OH$ (Hubler *et al.,* 2014). Moreover, ClO_2^- acts as redox couple with the other radiolysis product $ClO_2^{\bullet}$, via 1 e^- reduction (Stanbury and Lednicky, 1984) by, for example, $^{\bullet}OH$ [$ClO_2^- + {}^{\bullet}OH \rightarrow ClO_2^{\bullet} + OH^-$ (Klaning *et al.,* 1985)] or $O_2^{\bullet-}$ [$ClO_2^{\bullet} + O_2^{\bullet-} \rightarrow ClO_2^- + O_2$ (Huie and Neta, 1986)].

The source of residual O produced by radiolyzed perchlorate has been thought to be initially associated with

ClO_2 in the ClO_4^- ion and is not all available as gaseous O_2. Considerations of electrical neutrality would favor the simultaneous formation of a metal superoxide [thus $O_2^{\bullet-}$, being in the form of, *e.g.,* $Mg(O_2)_2$ (Bakulina *et al.,* 1970)], peroxide (*e.g.,* as MgO_2), or oxide (*e.g.,* as MgO) by the oxygen of ClO_2 (Prince and Johnson, 1965). $HO_2^{\bullet}$ and H_2O_2 generated by O atoms detached from radiolyzed aqueous ClO_4^- (resulting in the formation of ClO_3^-), presumably reduced via H attack, have been indirectly identified (using ions of iron, cerium, and thallium as scavengers) (Katakis and Allen, 1964; Katakis and Konstantatos, 1968). Another route for $O_2^{\bullet-}$ formation may be initiated by photoisomerization of $ClO_2^{\bullet}$ and its conversion to chloroperoxyl radicals ($ClOO^{\bullet}$) (Arkell and Schwager, 1967; Raghunathan and Sur, 1984). These upon reaction with $Cl^{\bullet}$ can be converted to chlorine monoxide radical ($ClO^{\bullet}$, via the reaction $ClO_2^{\bullet} + Cl^{\bullet} \rightarrow 2ClO^{\bullet}$) (Enami *et al.,* 2006), which, in turn, can react with $^{\bullet}OH$ and generate protonated superoxide radicals via the reaction $ClO^{\bullet} + {}^{\bullet}OH \rightarrow HO_2^{\bullet} + Cl^{\bullet}$ (Chang *et al.,* 2004), and recycle $Cl^{\bullet}$ for further production of $O_2^{\bullet-}$. Moreover, H_2O_2 can react with $^{\bullet}OH$ and generate protonated superoxide radicals via the reaction $H_2O_2 + {}^{\bullet}OH \rightarrow HO_2^{\bullet} + H_2O$ (Christensen *et al.,* 1982; Wang *et al.,* 2012). Other indirect mechanisms for H_2O_2 production could involve $^{\bullet}OH$ and $O_2^{\bullet-}$, both shown to be produced by radiolyzed ClO_4^- (Table 1), by $^{\bullet}OH$ fusion [$^{\bullet}OH + {}^{\bullet}OH \rightarrow H_2O_2$ (Lutze *et al.,* 2015)], and by dismutation of $O_2^{\bullet-}$, protonated or not [$2HO_2^{\bullet} \rightarrow 2H_2O_2 + O_2$ (Kurylo *et al.,* 1986) or $2O_2^{\bullet-} + 2H_2O \rightarrow 2OH^- + H_2O_2 + O_2$ (Georgiou *et al.,* 2015)].

Given that H_2O_2 was produced by both controls $NaClO_2$ and NaClO (Table 3), there could also be indirect sources of H_2O_2 that may produce it upon reaction with the various Cl-based products of perchlorate radiolysis such as ClO_2^- and ClO^-, free or both complexed with Mg [$Mg(ClO_2)_2 \cdot 6H_2O$ (Villars *et al.,* 2011) and MgClO (since thermally stable Mg^+ compounds are possible (Green *et al.,* 2007)), respectively].

Another possible source of O could have been either the radiolyzed CO_2 ($CO_2 \rightarrow CO + O$) (Lind and Bardwell, 1925; Harteck and Dondes, 1955; Watanabe *et al.,* 2007) that is present in the glass ampule of the radiolyzed samples, or the SiO_2 of the glass ampule itself. However, neither of these sources produced O that could react with the radiolyzed incomplete salt analogue and produce traceable ROS, because this salt analogue did not generate $O_2^{\bullet-}$ or H_2O_2 (Table 1). Moreover, the positive holes created in silica by γ radiation are irreversibly neutralized by H_2 (giving its characteristic color as they absorb at 320 and 530 nm) (Ogura *et al.,* 1974).

4.3. $^{\bullet}OH$ generation by radiolyzed $Mg(ClO_4)_2$ and Phoenix site salt analogue

Another important finding of the present study is that the Phoenix site salt analogue acts as a source of $^{\bullet}OH$ only upon γ radiolysis. Interestingly, $^{\bullet}OH$ is produced at quite high and near equal levels in the absence and presence of ClO_4^-, and it is still produced upon heating in both cases, although decreased by an average 2.5-fold (Table 1). On the other hand, the 6.9-fold increase in $^{\bullet}OH$ production by heated radiolyzed $Mg(ClO_4)_2$ compared to an unheated one suggests the generation in radiolyzed $Mg(ClO_4)_2$ of certain products that may act as scavengers of $^{\bullet}OH$. These products may be destroyed/modified and neutralized from reacting with $^{\bullet}OH$ (as they may do in the unheated sample, thereby decreasing its generated $^{\bullet}OH$ levels). Considering the possible sources of $^{\bullet}OH$ produced by the complete and the incomplete salt analogue, its ∼150-fold-high levels when compared to the 1 nmol $^{\bullet}OH$ produced by radiolyzed $Mg(ClO_4)_2$ suggest a minor contribution (∼0.7%) by the ClO_4^- portion in the complete salt analogue in the production of $^{\bullet}OH$. It is proposed that the production of almost all $^{\bullet}OH$ by the salt analogue ($\pm ClO_4^-$) is likely to be associated with the possible radiolysis of its SO_4^{2-} component. A possible mechanism may involve the production of sulfites (SO_3^{2}; together with elemental sulfur and sulfides), which can derive from SO_4^{2-} either in the presence of water ice [*e.g.,* in Europa (Carlson *et al.,* 2002)] or being in solid form [*e.g.,* Li_2SO_4 (Sasaki *et al.,* 1978)]. Sulfites could then generate $^{\bullet}OH$ (i) via oxidation by H_2O_2 (Shi, 1994; Shi *et al.,* 1994) detected in the present study [and also present on Mars (Encrenaz *et al.,* 2012)] or (ii) by autoxidation (together with sulfur trioxide anion radical, $SO_3^{\bullet-}$, generation) (Huie, 1986) in the presence of O_2 and H_2O [both also present on Mars, the first being possibly produced by radiolysis of perchlorate (Prince and Johnson, 1965; Quinn *et al.,* 2013)]. Given the presence of SO_4^{2-} at 134 nmol in 80 mg complete salt analogue (Quinn *et al.,* 2011), this concentration is comparable to the 149 nmol $^{\bullet}OH$ it generates upon radiolysis (Table 1). The other prone to radiolysis salt analogue component CO_3^{2-} is an unlikely source of $^{\bullet}OH$ because they react with each other to generate $^{\bullet}CO_3^-$ radicals (Haygarth *et al.,* 2010).

On the other hand, the minor contribution (0.7%) of $^{\bullet}OH$ due to the presence of ClO_4^- in the complete salt analogue could have originated from the reaction of $O_2^{\bullet-}$ with H_2O_2 [$O_2^{\bullet-} + H_2O_2 \rightarrow {}^{\bullet}OH + OH^- + O_2$ (Georgiou *et al.,* 2015)], both shown to be products of the radiolyzed complete salt analogue. This reaction may contribute to the release of O_2 by the H_2O-wetted radiolyzed perchlorate (Prince and Johnson, 1965; Quinn *et al.,* 2013). Although $O_2^{\bullet-}$ was not detected to be produced by radiolyzed $Mg(ClO_4)_2$ (but H_2O_2 was detected), its generation cannot be excluded because, as already mentioned, the generation of metal superoxides from γ-irradiated alkali and alkaline Earth perchlorate [and $Mg(ClO_4)_2$] has been predicted (Prince and Johnson, 1965). Therefore, these metal peroxidants upon H_2O wetting (thus dismutation) can become the source of the detected H_2O_2 (Table 1). Production of $^{\bullet}OH$ by the reaction between ClO^- and H_2O_2 at alkaline conditions ($ClO^- + H_2O_2 \rightarrow ClO^{\bullet} + OH + OH^-$) has also been suggested (Castagna *et al.,* 2008), but it does not seem to be the main mechanism because we were unable to demonstrate this using NaClO and H_2O_2.

Given the oxidizing effect of $NaClO_2$ and NaClO on 2HTPA (Fig. 2), the indirect quantifier (and trap) of $^{\bullet}OH$, the question arises whether ClO_2^- and ClO^- [expected radiolysis products of ClO_4^- (Prince and Johnson, 1965)] will affect the quantification of $^{\bullet}OH$ produced by the radiolyzed $Mg(ClO_4)_2$ and the complete salt analogue. Assuming that the radiolysis of 58.3 μmol ClO_4^- [as $Mg(ClO_4)_2$] generates ClO_2^-, ClO^-, and $ClO_2^{\bullet}$ at mol % concentration levels near equal to their $G°$ values [0.14, 0.03, and 0.07, respectively (Prince and Johnson, 1965)], these would correspond to approximately 80, 17, and 40 nmol, respectively, per 6.5 mg radiolyzed $Mg(ClO_4)_2$. Since $^{\bullet}OH$ production by the radiolyzed $Mg(ClO_4)_2$ alone and by the radiolyzed complete salt analogue was determined by the present study in these

samples at a 1–10 mg quantity range, their corresponding concentration in ClO_2^- and ClO^- would not have oxidized 2HTPA substantially (Fig. 2) enough to have caused an underestimation of the actual concentration of $^{\bullet}OH$. The oxidizing effect of $ClO_2^{\bullet}$ (the other presumed radiolysis product of ClO_4^-) on 2HTPA cannot be quantitatively assessed in the radiolyzed samples by commercial control analogues. However, it can be assumed to be minor due to the low (0.07) $G°$ value of $ClO_2^{\bullet}$.

4.4. Photolyzed ClO^- and ClO_2^- as potential sources of $^{\bullet}OH$, and its main generation mechanisms

Having established that $^{\bullet}OH$ is generated at high levels by radiolyzed Mars Phoenix site salt analogue (with and without perchlorate), the present study investigated a possible photogeneration mechanism for $^{\bullet}OH$ production by the ClO_4^- radiolysis products ClO^- and ClO_2 under simulated martian soil UV exposure conditions. Generation of $^{\bullet}OH$ was studied on NaClO and $NaClO_2$ by exposing them to low-UV-energy (thus time-controlled) photons (using UVA at flux density of 20 μW cm^{-2} up to 0.75 min exposure; Fig. 4), after having uncovered their oxychlorine products by UVC exposure at 1575 W m^{-2} up to 5 min exposure (Fig. 3). These doses are ~200-fold lower and 120-fold higher than the corresponding ones (41.5 and 13.2 W m^{-2}) that reach the surface of Mars at zenith angle 0° (Cockell *et al.,* 2000). Both NaClO and $NaClO_2$ produced $^{\bullet}OH$ at rates dependent on their concentration and UVA-photolysis exposure time period (Fig. 4). Production of $^{\bullet}OH$ by $NaClO_2$ is attributed to photolysis of UV-generated ClO^- (Fig. 3).

In hypothesizing the possible mechanisms of $^{\bullet}OH$ generation by ClO_4^--oxychlorine radiolysis products, the accuracy of measured $^{\bullet}OH$ was evaluated in relation to possible interfering factors. One factor is the possible oxidative effect of $NaClO_2$ and NaClO on 2HTPA fluorescence by which $^{\bullet}OH$ is indirectly quantified. It was concluded that this effect is insignificant at the low concentration levels of $NaClO_2$ and NaClO and short UVA exposure times studied (Fig. 2). Another possible factor affecting the actual production of $^{\bullet}OH$ by UV-photolyzed $NaClO_2$ could be the direct involvement of $^{\bullet}OH$ in the production of Cl_3^- (a UVC photolysis product of $NaClO_2$; Fig. 3) shown in Table 4. Another important factor is the accuracy of the 2HTPA-based $^{\bullet}OH$ standard curve used by the assay.

The involvement of the UV-photolyzed radiolysis products of perchlorate [at decreasing concentration sequence ClO_3^-, O_2, Cl^-, ClO_2^-, ClO^-, and $ClO_2^{\bullet}$ (Prince and Johnson, 1965)] in the production of $^{\bullet}OH$ requires an understanding of the photolysis and interconversion reactions involved, some of which release $^{\bullet}OH$ and others O_2 (Table 4). However, the most probable photolysis-induced $^{\bullet}OH$ production mechanism involves HOCl or ClO^- (Reactions 1a or 1b, the latter via the formation of an atomic oxygen radical anion, $O^{\bullet-}$, intermediate) (Wang *et al.,* 2012), and/or ClO_3^- (Reaction 2) (Osiewała *et al.,* 2013), as shown by the following corresponding reaction pathways:

1a. $HOCl + h\nu \rightarrow {}^{\bullet}OH + {}^{\bullet}Cl$

1b. $ClO^- + H_2O + h\nu \rightarrow {}^{\bullet}OH + {}^{\bullet}Cl + OH^-$

(1b is the sum of reactions: $ClO^- + h\nu \rightarrow {}^{\bullet}Cl + O^{\bullet-}$ and $O^{\bullet-} + H_2O \rightarrow {}^{\bullet}OH + OH^-$)

2. $ClO_3^- + H_2O + h\nu \rightarrow {}^{\bullet}OH + ClO_2^{\bullet} + OH^-$ (Osiewała et al., 2013)

The stoichiometry of the above reaction pathways predicts generation of 1 mol $^{\bullet}OH$ by 1 mol photolyzed ClO^-. However, our experiments with photolyzed NaClO showed that 7.6 and 23 nmol produced $^{\bullet}OH$ concentration plateaus at 16 and 45 nmol, respectively, which corresponds to a $ClO^-/{}^{\bullet}OH$ 1/2 molar stoichiometry (Fig. 4a). This finding can be explained by involving the reactions of the other photolysis product $^{\bullet}Cl$ (Cl atom) with H_2O or OH^- (Reaction 3a or 3b) (Lutze *et al.,* 2015), and $HO_2^{\bullet}$ (Reaction 4) (Chang *et al.,* 2004), which will produce the second mole of $^{\bullet}OH$ required for the $ClO^-/{}^{\bullet}OH$ molar ratio 1/2:

3a. With H_2O: $Cl^{\bullet} + H_2O \rightarrow {}^{\bullet}OH + Cl^- + H^+$

(3a is the sum of reactions: $Cl^{\bullet} + H_2O \rightarrow HClO^{\bullet-} + H^+$ and $HClO^{\bullet-} \rightleftarrows {}^{\bullet}OH + Cl^-$)

3b. With OH^-: $Cl^{\bullet} + OH^- \rightarrow {}^{\bullet}OH + Cl^-$

4. With $HO_2^{\bullet}$: $Cl^{\bullet} + HO_2^{\bullet} \rightarrow ClO^{\bullet} + {}^{\bullet}OH$

In turn, $^{\bullet}Cl$ and $^{\bullet}OH$ may be involved in reactions with the radiolysis products of perchlorate (Table 4).

Table 4. Interconversion Reactions of Radiolysis Products of Perchlorate

Involvement of $^{\bullet}OH$ in the production of Cl_3^-
Reaction mechanism (Paviet-Hartmann *et al.,* 2001)
$^{\bullet}OH + Cl^- (+Cl^-) \rightarrow Cl_2^- + OH^-$
$2Cl_2^- \rightarrow Cl_2 + 2Cl^-$ (or $Cl_3^- + Cl^-$)
Involving UV photolysis and release of $^{\bullet}OH$ and O_2
$ClO_2^- + h\nu \rightarrow ClO^{\bullet} + O^-$ (Osiewała *et al.,* 2013)
$O^- + ClO_2^- + H_2O \rightarrow ClO_2^{\bullet} + 2OH^-$ (Klaning *et al.,* 1985)
$O^- + ClO_2^{\bullet} \rightarrow ClO_3^-$ (Klaning *et al.,* 1985)
$ClO_2^{\bullet} + {}^{\bullet}OH \rightarrow ClO_3^- + H^+$ (Klaning *et al.,* 1985)
$^{\bullet}OCl + HO_2^{\bullet} \rightarrow HClO + O_2$ (Chang *et al.,* 2004)
$ClO_2^{\bullet} + O_2^{\bullet-} \rightarrow ClO_2^- + O_2$ (Huie and Neta, 1986)
$HClO + H_2O_2 \rightarrow H_2O + H^+ + Cl^- + O_2$ (Konstantatos and Katakis, 1967)
$2ClO^- \rightarrow 2Cl^- + O_2$ [uncatalyzed decomposition (Lister, 1956)]
Involving $Cl^{\bullet}$ and $^{\bullet}OH$
$Cl^{\bullet} + ClO^- \rightarrow ClO^{\bullet} + Cl^-$ (Buxton and Subhani, 1972; Kang *et al.,* 2006)
$ClO_2^{\bullet} + Cl^{\bullet} \rightarrow 2ClO^{\bullet}$ (Enami *et al.,* 2006)
$^{\bullet}OH + ClO_2^{\bullet} \rightarrow ClO_3^- + H^+$ (Klaning *et al.,* 1985)
$^{\bullet}OH + ClO_2^- \rightarrow ClO_2^{\bullet} + OH^-$ (Klaning *et al.,* 1985)
$^{\bullet}OH + ClO^{\bullet} \rightarrow HO_2^{\bullet} + Cl^{\bullet}$ (Chang *et al.,* 2004)
$^{\bullet}OH + Cl_2 \rightarrow HOCl + Cl^{\bullet}$ (Chang *et al.,* 2004)
$^{\bullet}OH + ClO^- \rightarrow ClO^{\bullet} + OH^-$ (Wang *et al.,* 2012; Lutze *et al.,* 2015)

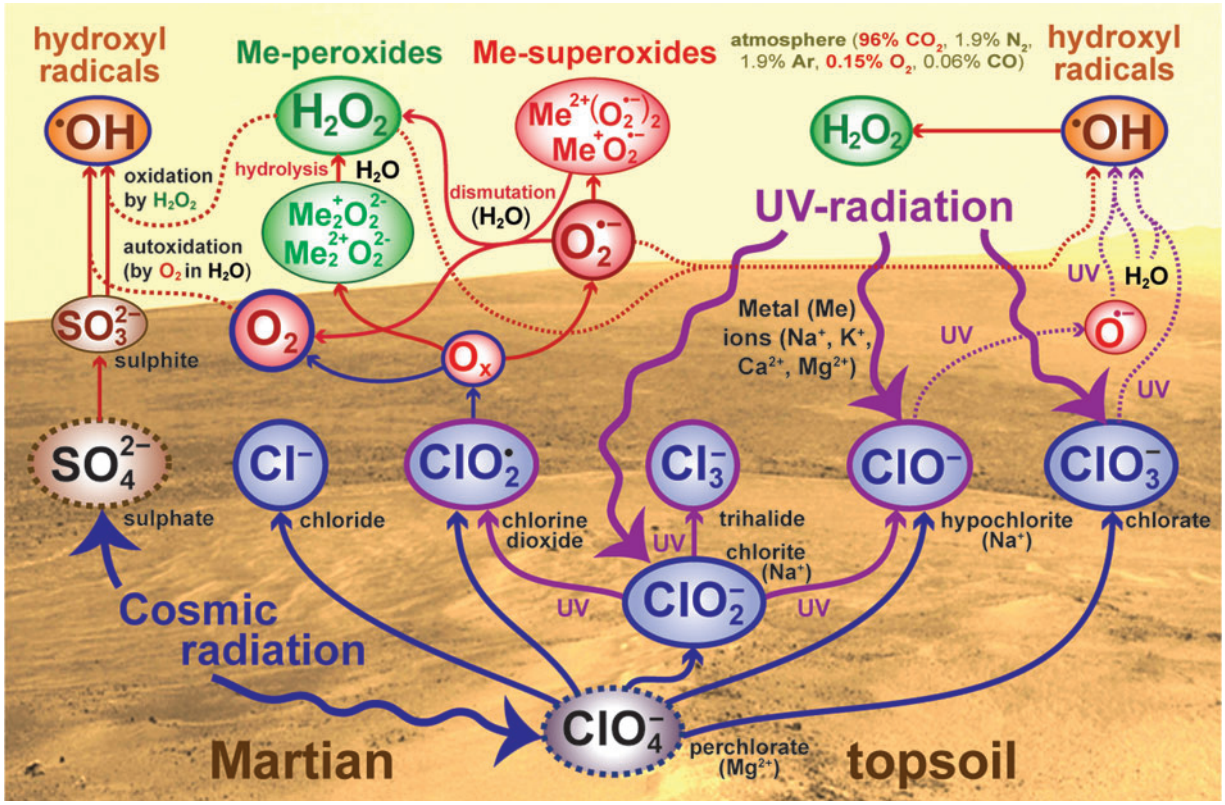

FIG. 5. Mechanisms of ROS generation by perchlorate and Mars Phoenix site salt analogue exposed to cosmic/UV radiation. Cosmic (γ) radiation decomposes perchlorate to ClO_3^-, O_2, Cl^-, ClO_2^-, ClO^-, and $ClO_2^{\bullet}$ (in a $G°$ value decreasing sequence) (Prince and Johnson, 1965), shown by solid arrows. Part of released residual O_x, associated with ClO_2 in the ClO_4^-, is matrix-trapped as gaseous O_2, while the other part is converted to $O_2^{\bullet-}$ (shown to be generated by the radiolyzed Mars Phoenix site complete salt analogue; Table 1), which in the presence of martian salt metal ions (Me) would favor the simultaneous formation of metal superoxides and peroxides (Katakis and Allen, 1964; Prince and Johnson, 1965; Katakis and Konstantatos, 1968). $O_2^{\bullet-}$ (free and present in metal superoxides) could dismutate to O_2 (an additional source of oxygen) and H_2O_2 (that could be also released by the hydrolysis of metal peroxides), which could then react with each other to generate $^{\bullet}OH$ (Georgiou *et al.,* 2015). Cosmic radiation could also radiolyze the salt analog component SO_4^{2-} to the intermediate sulfite, SO_3^{2-}, which upon oxidation by H_2O_2 (Shi, 1994; Shi *et al.,* 1994) or autoxidation (Huie, 1986) in the presence of H_2O and O_2 (released, *e.g.,* by radiolyzed ClO_4^-) will generate $^{\bullet}OH$ (as shown with the incomplete salt analogue, Table 1). Simultaneous UV photolysis of the ClO_4^- radiolysis product ClO_2^- produces additional ClO^- and $ClO_2^{\bullet}$, and also Cl_3^- (Fig. 3) as shown with dotted arrows. Then, upon UV photolysis, ClO^- (and ClO_2^- via ClO^-; Fig. 4) as well as ClO_3^- in the presence of H_2O will generate $^{\bullet}OH$ (ClO^- via the intermediate atomic oxygen radical anion, $O^{\bullet-}$), 2 mol of which can combine to produce 1 mol of H_2O_2.

4.5. Soil ROS on Mars

The present study suggests that martian topsoil is a continuous source of ROS generated by cosmic radiolysis and by a parallel UVA/C photolysis of ClO_2^- and ClO^-, both products of the cosmic radiolysis of ClO_4^-. The ClO_4^- radiolysis-H_2O-wetting-induced ROS generation mechanism (Fig. 5) originates from a Mars soil salt analogue (Phoenix site). This phenomenon may take place in parallel with another independent generation mechanism of soil ROS ($O_2^{\bullet-}$, H_2O_2, and secondarily $^{\bullet}OH$), by UV-induced electron ejection from soil mineral oxides and its subsequent trapping by O_2 as $O_2^{\bullet-}$ (Georgiou *et al.,* 2015), which is either released directly by radiolyzed ClO_4^- (Quinn *et al.,* 2013) or produced indirectly by the dismutation of $O_2^{\bullet-}$ that is also generated by radiolyzed ClO_4^- (Fig. 5).

The production of $^{\bullet}OH$ and H_2O_2 by radiolyzed ClO_4^- may contribute to the oxidative alteration of organics present in martian surface material. CO_2 can be produced by the reaction of organics with either H_2O_2 or $^{\bullet}OH$. H_2O_2 can decompose carbohydrates to formic acid and ultimately to CO_2 (Payne and Foster, 1945), while $^{\bullet}OH$ can produce CO_2 through various oxidation reactions with organics [*e.g.,* with methanol (Gehringer *et al.,* 1988; Munter, 2001) and with the products of oxidized organics carboxylic acids such as fumaric acid (Shi *et al.,* 2012)].

Considering the seasonality of the hydrated perchlorate-associated recurring slope lineae phenomenon (Ojha *et al.,* 2015) and the consequent periodic hydration of the ROS generating γ-radiolyzed/UV-photolyzed oxychlorine compounds and UV-radiated soil mineral oxides over short timescales, this raises the question of the potential lifetime of these ROS when wet. In such a case, ROS lifetime may be short and may not be an issue for habitability. On the other hand, surface water flows would also be exposed to UV when wet, which should generate ROS, perhaps

indicating poor preservation potential. Analyses of the martian surface performed with the SAM instrument on the Mars Science Laboratory have established the presence of significant quantities of organic matter (Ming *et al.,* 2014; Freissinet *et al.,* 2015). However, the chemical identities of the parent organic compounds present in the tested samples are obscured due to a thermal decomposition process induced by the presence of perchlorate (Ming *et al.,* 2014; Freissinet *et al.,* 2015). This points to the need for consideration of sample analysis methods in future missions. Although levels of ROS are expected to be low in comparison to perchlorate, sample cleanup processes (*e.g.,* solid phase extraction) or non-aqueous chemical derivatization may be required in the future prior to implementation of thermal or aqueous-based analysis methods. Additionally, analytical methods planned as part of the Mars Organic Molecule Analyzer (MOMA) on the upcoming ESA ExoMars mission include laser desorption mass spectroscopy (LDMS), which has been shown to be capable of the detection of trace organics in perchlorate-containing Mars analogues (Li *et al.,* 2015) and likewise should be compatible with the detection of organics in the presence of ROS-containing martian soils. The other instrument suitable for detection of organics, planned for the NASA Mars 2020 mission, is the Scanning Habitable Environments with Raman and Luminescence for Organics (SHERLOC) (Beegle *et al.,* 2014). SHERLOC uses a deep UV resonance Raman and fluorescence spectrometer utilizing a 248.6 nm deep UV laser for noncontact sample analysis. The technique may modify organics by inducing reactions with oxychlorine species (Beegle *et al.,* 2014). In light of the present study, modification of organics by ROS generated by UV irradiation of oxychlorine products may not be excluded. Moreover, UV bleaching may also be of concern.

The present study could partly explain the finding by the Curiosity rover of high Mn abundances (>25 wt % MnO) in fracture-filling materials that crosscut sandstones in the Kimberley region of Gale Crater of Mars (Lanza *et al.,* 2016), because their proposed accumulation as Mn-oxide deposits on Earth environments requires water and highly oxidizing conditions. The latter can be provided on Mars by the radiation-driven formation of ROS in the oxychlorine compounds of topsoil. Another possible source of ROS could be provided by the soil superoxides/peroxides that are possibly generated on Mars by the UV-irradiated topsoil, as they can be generated on Earth by UV-exposed arid desert soils (Georgiou *et al.,* 2015). The latter alternative ROS source and the fact that not all radiated oxychlorine products could produce ROS (Fig. 5) can explain the reported lack of correlation between Mn and the element Cl (Lanza *et al.,* 2016).

The impacts and distributions of ROS on the surface of Mars can be addressed in more specific terms by field instrumentation for the *in situ* detection and quantification of the metal superoxides ($O_2^{\bullet-}$) and peroxides (H_2O_2) present in martian topsoil. A methodology for the development of such an instrument is already available and is based on the enzymic/non-enzymic conversion of $O_2^{\bullet-}$ and H_2O_2 to stoichiometric O_2 (g) and, thus, their quantification by an O_2 electrode (Georgiou *et al.,* 2016).

To more faithfully recreate the cosmic ray particle bombardment onto the martian surface and near subsurface, similar irradiation experiments are planned using electron and proton bombardment combined with X-ray photoelectron spectroscopy analysis. For a more accurate simulation of martian soil, the Phoenix site salt analogue could be mixed with iron oxides, other oxides, and other expected soil components (*e.g.,* clays), which would likely affect the production (and chemistry) of the oxychlorine radiation-generated ROS. This is supported by the ~6-fold decreased rate of $^{\bullet}OH$ generation by H_2O extracts of desert soil compared to its absence (Georgiou *et al.,* 2015), possibly due to the scavenging action of metal (Me) ions [$^{\bullet}OH + Me^{n+}H_2O \rightarrow Me^{n+}OH \rightarrow Me^{(n+1)+} + OH^-$ (Buxton *et al.,* 1988)].

4.6. Relationships to the Viking LR and GEx experiments

Our results show that radiolysis of $Mg(ClO_4)_2$ in a 7 torr CO_2 atmosphere produces peroxide, but not superoxide. $^{\bullet}OH$ is also produced presumably due to trace amounts of water associated with the $Mg(ClO_4)_2$ sample. Heat treatment of the sample prior to analysis resulted in a >98% decrease in peroxide concentration and a corresponding increase (number of moles) in $^{\bullet}OH$. In the Viking GEx experiments, the production of 70–700 nmol of O_2 (g) was measured when martian surface samples were humidified or wetted (Oyama and Berdahl, 1977). The total quantity of ROS sum (O_2^{2-}, $O_2^{\bullet-}$, and $^{\bullet}OH$) measured in the irradiated (500 kGy) $Mg(ClO_4)_2$ (without Phoenix salt analogue) in this study totaled ~7 nmol. However, the 1 nmol of $^{\bullet}OH$ measured is not an accurate representation of the $^{\bullet}OH$ content. The reason for this is that $^{\bullet}OH$ is indirectly quantified (via scavenging by TPA). Therefore, we estimate (data not shown) that the level of $^{\bullet}OH$ in the sample is ~30 nmol and that the total quantity of ROS in the sample is closer to the lower end of the range of O_2 (g) levels observed in the Viking GEx experiment (70–700 nmol), assuming similar levels of perchlorate at both the Viking and Phoenix sites. Importantly, the amount of ROS (primarily $^{\bullet}OH$) measured in the Phoenix salt (without perchlorate) analogue was within the range of O_2 (g) levels. Along with the observed thermal stability, this points to the likely extensive formation of ROS on the surface of Mars across diverse mineral matrices, which suggests that there may be additional sources of oxygen [*e.g.,* SO_4^{2-}, soil mineral oxides (Georgiou *et al.,* 2015)] that may have contributed to the GEx O_2 (g) releases. It should be noted, though, that the kinetics of O_2 (g) formation from $^{\bullet}OH$ humidification or wetting was not examined in the present study. Additionally, the amount of ROS measured in our experiments represents only a small fraction of the total free oxygen produced by perchlorate radiolysis. The ROS mol % fraction measured relative to total $Mg(ClO_4)_2$ in the current study was 0.01. In contrast, Quinn *et al.* (2013) measured a 1 mol % fraction of O_2 (g) released from irradiated (500 kGy) $Ca(ClO_4)_2$ upon sample wetting. The expected total amount of free oxygen produced in the γ-irradiated $Mg(ClO_4)_2$ examined in this study is ~2 μmol, based on a G° value of 2.62 (Prince and Johnson, 1965), which correlates to a measured ROS mol % fraction of 0.4 (relative to the expected total oxygen production measured as O_2). While this may imply that ultimately the majority of oxygen produced by perchlorate radiolysis is stabilized and trapped in, or released from, the perchlorate as

O_2 (g), our results suggest that radiolysis pathways dictate that the formation of O_2 (g) occurs via ROS metastable intermediates, which ultimately form, and coexist, with trapped O_2 (g). The significance of this is that the ROS formed during radiolysis of martian surface materials may not only serve as the soil O_2 precursor that ultimately was measured as O_2 (g) in the Viking GEx experiment, but also, due to their high reactivity, likely act to chemically alter both the mineral and organic fractions of martian surface materials *in situ*.

In the Viking LR experiments, when 0.5 cc of surface soil material was wetted with an aqueous nutrient media that contained ^{14}C-labeled organics, $\sim$30 nmol of ^{14}C-labeled gas (presumably $^{14}CO_2$) was released into the LR test cell headspace (Levin and Straat, 1977). Table 1 shows that the levels of H_2O_2 and $O_2^{\bullet-}$ produced in our experiments were lower than the $\sim$30 nmol ^{14}C-release observed in the Viking LR, but more importantly these samples were not tested to demonstrate that they reproduced the kinetics of the LR ^{14}C-gas release. Production of $^{\bullet}$OH in the irradiated Phoenix salt analogues (both with or without perchlorate) can be discounted as a possible explanation of the LR experiment due to its thermal stability. However, assuming that production of low levels of H_2O_2 by heated radiolyzed $Ca(ClO_4)_2$ is similar to those produced by heated radiolyzed $Mg(ClO4)_2$ (61-fold decreased H_2O_2 production of heated over unheated; Table 1), these very low H_2O_2 levels (and possibly low levels of $^{\bullet}$OH) may contribute to CO_2 production, although not at levels seen in the $Ca(ClO_4)_2$ radiolysis study (Quinn *et al.,* 2013) that resulted from the formation and spontaneous decomposition of chloroaniline.

An important finding of the current study is the reduced recovery (55.6%) of ClO^- after heating NaClO (water removal at 20–50°C) and a 97% reduction in ClO^- recovery after heating NaClO for 3 h at 160°C). Levin and Straat (2016) pointed out that Quinn *et al.* (2013) did not attempt to demonstrate that hypochlorite matches the observed thermal stability profile of the LR oxidant. In the Viking LR experiment, the magnitude of the $^{14}CO_2$ release was reduced by $\sim$70% when heated to 46°C for 3 h and was nearly completely eliminated when heated to 51°C for 3 h. Although the current results do not offer a perfect match to the Viking LR, these experiments were not designed to be a rigorous test of LR results. The results do show, however, that the thermal stability profile of NaClO is in the range of what was observed in the LR experiment. Further experiments are planned to characterize the thermal stability of hypochlorite and other oxychlorine species in the context of the LR experiments.

5. Conclusions

The present study shows that γ-radiolyzed $Mg(ClO_4)_2$ alone generates H_2O_2 and hydroxyl radicals ($^{\bullet}$OH) upon H_2O wetting. On the other hand, the γ-radiolyzed complete Mars Phoenix site salt analogue [containing $Mg(ClO_4)_2$] generates $O_2^{\bullet-}$, H_2O_2, and $^{\bullet}$OH, the latter at 150-fold higher concentration than that generated by $Mg(ClO_4)_2$ alone. Radiolyzed Mars Phoenix site salt analogue depleted of $Mg(ClO_4)_2$ generates only $^{\bullet}$OH, at 150-fold higher concentration than by $Mg(ClO_4)_2$ alone, and at equal concentration with the complete Mars Phoenix site salt analogue, suggesting the radiolyzed salt analog component SO_4^{2-} as the most probable source of $^{\bullet}$OH. Perchlorate γ-radiolysis product chlorite (ClO_2^-) under UV exposure and upon H_2O wetting generates the oxychlorine products trihalide (Cl_3^-), chlorine dioxide radical ($ClO_2^{\bullet}$), and hypochlorite (ClO^-), with the latter acting as $^{\bullet}$OH source when UV photolyzed and upon H_2O wetting.

Acknowledgments

The Greek Ministry of Education financially supported this work. R.Q. acknowledges the support of the NASA Astrobiology Institute.

Author Disclosure Statement

No competing financial interests exist.

References

Arkell, A. and Schwager, I. (1967) A matrix isolation study of the ClOO radical. *J Am Chem Soc* 89:5999–6006.

Bakulina, V.M., Tokareva, S.A., Latysheva, E.I., and Vol'nov, I.I. (1970) X-ray diffraction study of magnesium superoxide $Mg(O_2)_2$. *J Struct Chem* 11:150–151.

Beegle, L.W., Bhartia, R., DeFlores, L., Darrach, M., Kidd, R.D., Abbey, W., Asher, S., Burton, A., Clegg, S., Conrad, P.G., Edgett, K.S., Ehlmann, B.L., Langenhorst, F., Fries, M., Nealson, K.H., Popp, J., Sobron, P., Steele, A., Wiens, R.C., and Williford, K.H. (2014) SHERLOC: Scanning Habitable Environments with Raman & Luminescence for Organics & Chemicals, an investigation for 2020. In *GeoRaman 2014,* 11th International GeoRaman Conference, St. Louis, MO.

Biemann, K., Oro, J., Toulmin, P., III, Orgel, L.E., Nier, A.O., Anderson, D.M., Simmonds, P.G., Flory, D., Diaz, A.V., Rushneck, D.R., and Simmonds, P.G. (1977) The search for organic substances and inorganic volatile compounds in the surface of Mars. *J Geophs Res* 82:4641–4658.

Buxton, G.V. and Subhani, M.S. (1972) Radiation chemistry and photochemistry of oxychlorine ions. Part 2.—Photodecomposition of aqueous solutions of hypochlorite ions. *Journal of the Chemical Society, Faraday Transactions 1: Physical Chemistry in Condensed Phases* 68:958–969.

Buxton, G.V., Greenstock, C.L., Helman, W.P., and Ross, A.B. (1988) Critical review of rate constants for reactions of hydrated electrons, hydrogen atoms and hydroxyl radicals (OH/O) in aqueous solution. *J Phys Chem Ref Data* 17:513–886.

Carlson, R.W., Anderson, M.S., Johnson, R.E., Schulman, M.B., and Yavrouian, A.H. (2002) Sulfuric acid production on Europa: the radiolysis of sulfur in water ice. *Icarus* 157:456–463.

Carrier, B.L. and Kounaves, S.P. (2015) The origins of perchlorate in the martian soil. *Geophys Res Lett* 42:3746–3754.

Castagna, R., Eiserich, J.P., Budamagunta, M.S., Stipa, P., Cross, C.E., Proietti, E., Voss, J.C., and Greci, L. (2008) Hydroxyl radical from the reaction between hypochlorite and hydrogen peroxide. *Atmos Environ* 42:6551–6554.

Catling, D.C., Cockell, C.S., and McKay, C.P. (1999) Ultraviolet radiation on the surface of Mars [abstract 6128]. In *Fifth International Conference on Mars,* Lunar and Planetary Science Institute, Houston.

Catling, D.C., Claire, M.W., Zahnle, K.J., Quinn, R.C., Clark, B.C., Hecht, M.H., and Kounaves, S. (2010) Atmospheric origins of perchlorate on Mars and in the Atacama. *J Geophys Res* 115, doi:10.1029/2009JE003425.

Chang, C.-T., Liu, T.-H., and Jeng, F.-T. (2004) Atmospheric concentrations of the Cl atom, ClO radical, and HO radical in the coastal marine boundary layer. *Environ Res* 94:67–74.

Christensen, H., Sehested, K., and Corfitzen, H. (1982) Reactions of hydroxyl radicals with hydrogen peroxide at ambient and elevated temperatures. *J Phys Chem* 86:1588–1590.

Chun, S.F.S., Pang, K.D., Cutts, J.A., and Ajello, J.M. (1978) Photocatalytic oxidation of organic compounds on Mars. *Nature* 274:875–876.

Cockell, C.S., Catling, D.C., Davis, W.L., Snook, K., Kepner, R.L., Lee, P., and McKay, C.P. (2000) The ultraviolet environment of Mars: biological implications past, present, and future. *Icarus* 146:343–359.

Elsenousy, A. and Chevrier, V. (2014) Thermodynamic properties of hypochlorites and chlorites: applications to the Phoenix surface [abstract 2920]. In *45th Lunar and Planetary Science Conference,* Lunar and Planetary Science Institute, Houston.

Enami, S., Hoshino, Y., Ito, Y., Hashimoto, S., Kawasaki, M., and Wallington, T.J. (2006) Kinetic study of the ClOO + NO reaction using cavity ring-down spectroscopy. *J Phys Chem A* 16:3546–3551.

Encrenaz, T., Greathouse, T.K., Lefèvre, F., and Atreya, S.K. (2012) Hydrogen peroxide on Mars: observations, interpretation and future plans. *Planet Space Sci* 68:3–17.

Freissinet, C., Glavin, D.P., Mahaffy, P.R., Miller, K.E., Eigenbrode, J.L., Summons, R.E., Brunner, A.E., Buch, A., Szopa, C., Archer, P.D., Jr., Franz, H.B., Atreya, S.K., Brinckerhoff, W.B., Cabane, M., Coll, P., Conrad, P.G., Des Marais, D.J., Dworkin, J.P., Fairén, A.G., François, P., Grotzinger, J.P., Kashyap, S., ten Kate, I.L., Leshin, L.A., Malespin, C.A., Martin, M.G., Martin-Torres, J.F., McAdam, A.C., Ming, D.W., Navarro-González, R., Pavlov, A.A., Prats, B.D., Squyres, S.W., Steele, A., Stern, J.C., Sumner, D.Y., Sutter, B., Zorzano, M.-P.; MSL Science Team. (2015) Organic molecules in the Sheepbed Mudstone, Gale Crater, Mars. *J Geophys Res: Planets* 120:495–514.

Gehringer, P., Proksch, E., Szinovatz, W., and Eschweiler, H. (1988) Radiation-induced decomposition of aqueous trichloroethylene solutions. *Int J Rad Appl Instrum A* 39:1227–1231.

Georgiou, C.D., Sun, H.J., McKay, C.P., Grintzalis, K., Papapostolou, I., Zisimopoulos, D., Panagiotidis, K., Zhang, G., Koutsopoulou, E., Christidis, G.E., and Margiolaki, I. (2015) Evidence for photochemical production of reactive oxygen species in desert soils. *Nat Commun* 6, doi:10.1038/ncomms8100.

Georgiou, C.D., Zisimopoulos, D., Panagiotidis, K., Grintzalis, K., Papapostolou, I., Quinn, R.C., McKay, C.P., and Sun, H. (2016) Martian superoxide and peroxide O_2 release (OR) assay: a new technology for terrestrial and planetary applications. *Astrobiology* 16:126–142.

Glavin, D.P., Freissinet, C., Miller, K.E., Eigenbrode, J.L., Brunner, A.E., Buch, A., Sutter, B., Archer, P.D.J., Atreya, S.K., Brinckerhoff, W.B., Cabane, M., Coll, P., Conrad, P.G., Coscia, D., Dworkin, J.P., Franz, H.B., Grotzinger, J.P., Leshin, L.A., Martin, M.G., McKay, C., Ming, D.W., Navarro-González, R., Pavlov, A., Steele, A., Summons, R.E., Szopa, C., Teinturier, S., and Mahaffy, P.R. (2013) Evidence for perchlorates and the origin of chlorinated hydrocarbons detected by SAM at the Rocknest aeolian deposit in Gale Crater. *J Geophs Res* 118:1955–1973.

Green, S.P., Jones, C., and Stasch, A. (2007) Stable magnesium(I) compounds with Mg-Mg bonds. *Science* 318:1754–1757.

Grintzalis, K., Zisimopoulos, D., Grune, T., Weber, D., and Georgiou, C.D. (2013) Method for the simultaneous determination of free/protein malondialdehyde and lipid/protein hydroperoxides. *Free Radic Biol Med* 59:27–35.

Halliwell, B. and Gutteridge, C.M.J. (1999) *Free Radicals in Biology and Medicine,* Oxford University Press, Oxford, UK.

Harteck, P. and Dondes, S. (1955) Decomposition of carbon dioxide by ionizing radiation. Part I. *J Chem Phys* 23:902–908.

Hassler, D.M., Zeitlin, C., Wimmer-Schweingruber, R.F., Ehresmann, B., Rafkin, S., Eigenbrode, J.L., Brinza, D.E., Weigle, G., Böttcher, S., Böhm, E., Burmeister, S., Guo, J., Köhler, J., Martin, C., Reitz, G., Cucinotta, F.A., Kim, M.H., Grinspoon, D., Bullock, M.A., Posner, A., Gómez-Elvira, J., Vasavada, A., Grotzinger, J.P.; MSL Science Team. (2014) Mars' surface radiation environment measured with the Mars Science Laboratory's Curiosity Rover. *Science* 343, doi:10.1126/science.1244797.

Haygarth, K.S., Marin, T.M., Janik, I., Kanjana, K., Stanisky, C.M., and Bartels, D.M. (2010) Carbonate radical formation in radiolysis of sodium carbonate and bicarbonate solutions up to 250°C and the mechanism of its second order decay. *J Phys Chem A* 114:2142–2150.

Hecht, M.H., Kounaves, S.P., Quinn, R.C., West, S.J., Young, S.M.M., Ming, D.W., Catling, D.C., Clark, B.C., Boynton, W.V., Hoffman, J., Deflores, L.P., Gospodinova, K., Kapit, J., and Smith, P.H. (2009) Detection of perchlorate and the soluble chemistry of martian soil at the Phoenix lander site. *Science* 325:64–67.

Hubler, D.K., Baygents, J.C., Chaplin, B.P., and Farrell, J. (2014) Understanding chlorite and chlorate formation associated with hypochlorite generation at boron doped diamond film anodes. *J Electrochem Soc* 161:E182–E189.

Huie, R.E. (1986) Chemical kinetics of intermediates in the autoxidation of SO_2. In *Fossil Fuels Utilization: Environmental Concerns,* edited by R. Markuszewski and B.D. Blausteins, American Chemical Society, Washington, DC, pp 284–292.

Huie, R.E. and Neta, P. (1986) Kinetics of one-electron transfer reactions involving ClO_2 and NO_2. *J Phys Chem* 90:1193–1198.

Kang, N., Anderson, T.A., and Jackson, W.A. (2006) Photochemical formation of perchlorate from aqueous oxychlorine anions. *Anal Chim Acta* 567:48–56.

Katakis, D. and Allen, O.A. (1964) The radiolysis of aqueous perchloric acid solutions. *J Phys Chem* 68:3107–3115.

Katakis, D. and Konstantatos, J. (1968) Decomposition of aqueous perchlorates by radiation. *J Phys Chem* 72:2054–2057.

Klaning, U.K., Sehested, K., and Holcman, J. (1985) Standard Gibbs energy of formation of the hydroxyl radical in aqueous solution. Rate constants for the reaction chlorite (ClO_2^-) + ozone .dblarw. ozone(1-) + chlorine dioxide. *J Phys Chem* 89:760–763.

Klein, H.P., Horowitz, N.H., Levin, G.V., Oyama, V.I., Lederberg, J., Rich, A., Hubbard, J.S., Hobby, G.L., Straat, P.A., Berdahl, B.J., Carle, G.C., Brown, F.S., and Johnson, R.D. (1976) The Viking biological investigation: preliminary results. *Science* 194:99–105.

Konstantatos, J. and Katakis, D. (1967) The radiolysis of concentrated neutral sodium perchlorate aqueous solutions. *J Phys Chem* 71:979–983.

Kurylo, M.J., Ouellette, P.A., and Laufer, A.H. (1986) Measurements of the pressure dependence of the HO_2 radical self-disproportionation reaction at 298 K. *J Phys Chem* 90:437–440.

Lanza, N.L., Wiens, R.C., Arvidson, R.E., Clark, B.C., Fischer, W.W., Gellert, R., Grotzinger, J.P., Hurowitz, J.A., McLennan, S.M., Morris, R.V., Rice, M.S., Bell, J.F., Berger, J.A., Blaney, D.L., Bridges, N.T., Calef, F., Campbell, J.L., Clegg, S.M., Cousin, A., Edgett, K.S., Fabre, C., Fisk, M.R., Forni, O., Frydenvang, J., Hardy, K.R., Hardgrove, C., Johnson, J.R., Lasue, J., Le Mouélic, S., Malin, M.C., Mangold, N.,

Martın-Torres, J., Maurice, S., McBride, M.J., Ming, D.W., Newsom, H.E., Ollila, A.M., Sautter, V., Schröder, S., Thompson, L.M., Treiman, A.H., VanBommel, S., Vaniman, D.T., and Zorzano, M.-P. (2016) Oxidation of manganese in an ancient aquifer, Kimberley Formation, Gale Crater, Mars. *Geophys Res Lett* 43, doi:10.1002/2016GL069109.

Levin, G.V. and Straat, P.A. (1977) Recent results from the Viking Labeled Release Experiment on Mars. *J Geophys Res* 82:4663–4667.

Levin, G.V. and Straat, P.A. (2016) The case for extant life on Mars and its possible detection by the Viking Labeled Release Experiment. *Astrobiology* 16:798–810.

Li, X., Brinckerhoff, W.B., Pinnick, V.T., van Amerom, F.H.W., Danell, R.M., Arevalo, R.D.J., Getty, S., and Mahaffy, P.R. (2015) *In situ* detection of organic molecules on the martian surface with the Mars Organic Molecule Analyzer (MOMA) on ExoMars 2018 [abstract 7451]. In *Astrobiology Science Conference 2015,* Lunar and Planetary Institute, Houston.

Liao, C.H., Kang, S.-F., and Wu, F.A. (2001) Hydroxyl radical scavenging role of chloride and bicarbonate ions in the H_2O_2/UV process. *Chemosphere* 44:1193–1200.

Lind, S.C. and Bardwell, D.C. (1925) The chemical action of gaseous ions produced by alpha particles.[1] VI.[2] Reactions of the oxides of carbon. *J Am Chem Soc* 47:2675–2697.

Lister, M.W. (1956) Decomposition of sodium hypochlorite: the uncatalyzed reaction. *Can J Chem* 34:465–478.

Lutze, H.V., Kerlin, N., and Schmidt, T.C. (2015) Sulfate radical-based water treatment in presence of chloride: formation of chlorate, inter-conversion of sulfate radicals into hydroxyl radicals and influence of bicarbonate. *Water Res* 72:349–360.

Ming, D.W., Archer, P.D., Jr., Glavin, D.P., Eigenbrode, J.L., Franz, H.B., Sutter, B., Brunner, A.E., Stern, J.C., Freissinet, C., McAdam, A.C., Mahaffy, P.R., Cabane, M., Coll, P., Campbell, J.L., Atreya, S.K., Niles, P.B., Bell, J.F., III, Bish, D.L., Brinckerhoff, W.B., Buch, A., Conrad, P.G., Des Marais, D.J., Ehlmann, B.L., Fairén, A.G., Farley, K., Flesch, G.J., Francois, P., Gellert, R., Grant, J.A., Grotzinger, J.P., Gupta, S., Herkenhoff, K.E., Hurowitz, J.A., Leshin, L.A., Lewis, K.W., McLennan, S.M., Miller, K.E., Moersch, J., Morris, R.V., Navarro-González, R., Pavlov, A.A., Perrett, G.M., Pradler, I., Squyres, S.W., Summons, R.E., Steele, A., Stolper, E.M., Sumner, D.Y., Szopa, C., Teinturier, S., Trainer, M.G., Treiman, A.H., Vaniman, D.T., Vasavada, A.R., Webster, C.R., Wray, J.J., Yingst, R.A.; MSL Science Team. (2014) Volatile and organic compositions of sedimentary rocks in Yellowknife Bay, Gale Crater, Mars. *Science* 343, doi:10.1126/science.1245267.

Munter, R. (2001) Advanced oxidation processes: current status and prospects. *Proceedings of the Estonian Academy of Sciences. Chemistry* 50:59–80.

Navarro-González, R., Vargas, E., de la Rosa, J., Raga, A.C., and McKay, C.P. (2010) Reanalysis of the Viking results suggests perchlorate and organics at mid-latitudes on Mars. *J Geophys Res* 115, doi:10.1029/2010JE003599.

Ogura, H., Tachika, Y., Suzuki, Y., Nakazato, C., Kondo, M., Sawai, T., and Sawai, T. (1974) Effect of gamma radiation on silica gel. *J Nucl Sci Technol* 12:167–173.

Ojha, L., Wilhelm, M.B., Murchie, S.L., McEwen, A.S., Wray, J.J., Hanley, J., Massé, M., and Chojnacki, M. (2015) Spectral evidence for hydrated salts in recurring slope lineae on Mars. *Nat Geosci* 8:829–832.

Osiewała, L., Socha, A., Perek, A., Socha, M., and Rynkowski, J. (2013) Electrochemical, photochemical, and photoelectrochemical treatment of sodium *p*-cumenesulfonate. *Water Air Soil Pollut* 224, doi:10.1007/s11270-013-1657-3.

Oyama, V.I. and Berdahl, B.J. (1977) The Viking Gas Exchange experiment results from Chryse and Utopia surface samples. *J Geophys Res* 82:4669–4676.

Oyama, V.I., Berdahl, B.J., and Carle, G.C. (1977) Preliminary findings of the Viking Gas Exchange Experiment and a model for martian surface chemistry. *Nature* 265:110–114.

Paviet-Hartmann, P., Dziewinski, J., Hartmann, T., Marczak, S., Lu, N., Walthall, M., Rafalski, A., and Zagorski, Z.P. (2001) Spectroscopic investigation of the formation of radiolysis by-products by 13/9 MeV Linear Accelerator of Electrons (LAE) in salt solutions. In *WM'02 Conference,* INIS, Tucson, AZ, pp 1–10.

Pavlov, A.K., Blinov, A.V., and Konstantinov, A.N. (2002) Sterilization of martian surface by cosmic radiation. *Planet Space Sci* 50:669–673.

Payne, H.J. and Foster, L. (1945) The action of hydrogen peroxide on carbohydrates. *J Am Chem Soc* 67:1654–1656.

Prince, L.A. and Johnson, E.R. (1965) The radiation-induced decomposition of the alkali and alkaline Earth perchlorates. I. Product yields and stoichiometry. *J Phys Chem* 69:359–377.

Quinn, R.C. and Zent, A.P. (1999) Peroxide-modified titanium dioxide: a chemical analog for putative martian soil oxidants. *Orig Life Evol Biosph* 29:59–72.

Quinn, R.C., Chittenden, J.D., Kounaves, S.P., and Hecht, M.H. (2011) The oxidation-reduction potential of aqueous soil solutions at the Mars Phoenix landing site. *Geophys Res Lett* 38:L14202.

Quinn, R.C., Martucci, H.F., Miller, S.R., Bryson, C.E., Grunthaner, F.J., and Grunthaner, P.J. (2013) Perchlorate radiolysis on Mars and the origin of martian soil reactivity. *Astrobiology* 13:515–520.

Raghunathan, P. and Sur, S.K. (1984) EPR study of the chloroperoxy radical, ClOO, stabilized in the zeolitic host matrix of cancrinite. *J Am Chem Soc* 106:8014–8017.

Sasaki, T., Williams, R.S., Wong, J.S., and Shirley, D.A. (1978) Radiation damage studies by X-ray photoelectron spectroscopy. I. Electron irradiated $LiNO_3$ and Li_2SO_4. *J Chem Phys* 68:2718–2724.

Shi, L., Wang, X., Li, N., Huai, C., and Liu, J. (2012) UV irradiation chlorine dioxide photocatalytic oxidation of simulated fuchsine wastewater by UV-vis and online FTIR spectrophotometric method. *ISRN Analytical Chemistry* 2012, doi:10.5402/2012/951465.

Shi, X. (1994) Generation of $SO_3^{\bullet-}$ and OH radicals in SO_3^{2-} reactions with inorganic environmental pollutants and its implications to SO_3^{2-} toxicity. *J Inorg Biochem* 56:155–165.

Shi, X., Dalal, N., and Kasprzak, K.S. (1994) Enhanced generation of hydroxyl radical and sulfur trioxide anion radical from oxidation of sodium sulfite, nickel(II) sulfite, and nickel subsulfide in the presence of nickel(II) complexes. *Environ Health Perspect* 102(Suppl 3):91–96.

Stanbury, D.M. and Lednicky, L.A. (1984) Outer-sphere electron-transfer reactions involving the chlorite/chlorine dioxide couple. Activation barriers for bent triatomic species. *J Am Chem Soc* 106:2847–2853.

Villars, P., Cenzual, K., Daams, J., Gladyshevskii, R., Shcherban, O., Dubenskyy, V., Kuprysyuk, V., Savysyuk, I., and Zaremba, R. (2011) $Mg(ClO_2)_2 \cdot 6H_2O$. In *Structure Types. Part 10: Space Groups (140) I4/mcm–(136) $P4_2/mnm$*, Springer, Berlin, p 736.

Wang, D., Bolton, J.R., and Hofmann, R. (2012) Medium pressure UV combined with chlorine advanced oxidation for

trichloroethylene destruction in a model water. *Water Res* 46:4677–4686.

Watanabe, D., Yoshida, T., Allen, C., and Tanabe, T. (2007) Enhancement of gamma-ray radiolysis of carbon dioxide with the assistance of solid materials. *J Radioanal Nucl Chem* 272:461–465.

Yen, A.S., Kim, S.S., Hecht, M.H., Frant, M.S., and Murray, B. (2000) Evidence that the reactivity of the martian soil is due to superoxide ions. *Science* 289:1909–1912.

Address correspondence to:
Christos D. Georgiou
Department of Biology
University of Patras 26504
Greece

E-mail: c.georgiou@upatras.gr

Submitted 17 May 2016
Accepted 3 November 2016

Abbreviations Used

2HTPA = 2-hydroxy terephthalic acid
ACN = acetonitrile
ACN_{alk} = alkaline acetonitrile
CAT = catalase
CE = dicyclohexano-18-crown-6 ether
DMSO = dimethyl sulfoxide
FU = fluorescence units
GCMS = Gas Chromatograph Mass Spectrometer
GEx = Gas Exchange
HE = hydroethidine
LR = Labeled Release
ROS = reactive oxygen species
SAM = Sample Analysis at Mars
SHERLOC = Scanning Habitable Environments with Raman and Luminescence for Organics
TPA = terephthalic acid